52

Anisotropic dielectric waveguides

M. Lu and M. M. Fejer

Edward L. Ginzton Laboratory, Stanford University, Stanford, California 94305

Received September 5, 1991; accepted June 1, 1992; revised manuscript received August 7, 1992

The guided modes of anisotropic waveguides are known to be leaky when degenerate radiation modes of the orthogonal polarization exist. These losses can be quite large when the principal axes of the dielectric tensor are not aligned with the waveguide axis. We calculate the leakage rate in waveguides that have arbitrarily oriented dielectric tensors, using a perturbation expansion that is valid for weak guidance and weak anisotropy. A relatively simple expression for the loss is obtained and is applied to model cases drawn from planar and fiber waveguides with step- and graded-index profiles. The scaling of the loss with profile height and anisotropy is discussed, including the practical case of strongly asymmetric planar waveguides.

1. INTRODUCTION

It is well known that modes that are polarized along the fast axis of an anisotropic waveguide are in many cases leaky. The leakage is caused by the coupling of the guided mode to nearly degenerate radiation modes of the orthogonal polarization. Such degenerate modes exist whenever the birefringence of the waveguide exceeds the index difference between the core and the cladding, and coupling between modes occurs if they are not linearly polarized along principal axes of the dielectric tensor. In planar waveguides the latter condition holds only when certain off-diagonal elements of the dielectric tensor are nonzero. However, coupling is always present in two-dimensional waveguides, because the true modes are not linearly polarized. If, in addition, the off-diagonal elements of the dielectric tensor are nonzero, stronger coupling can occur.

The leakage that is due to stress-induced birefringence has been used in the design of single-polarization glass fibers.[1] In anisotropic crystalline waveguides, such leakage can be orders of magnitude larger and often precludes propagation in directions that are of interest for applications, particularly in nonlinear devices. A number of analyses of the leakage loss in planar structures have been published, including an exact solution of the symmetric[2] and the asymmetric[3,4] planar waveguides, a WKB method,[5,6] a coupled-mode method,[7] and a multilayer numerical approximation.[8]

Snyder and Ruhl[1] presented a useful weakly guiding perturbation method for a step-profile anisotropic fiber in which one of the principal axes of the dielectric tensor aligned with the waveguide axis. Later Ruhl and Snyder[9] demonstrated a Green function method for the same problem. The leaky modes in fibers in which the principal axes in both the core and the cladding were aligned with the waveguide axis but were misaligned with each other in the transverse plane are discussed in Ref. 10.

In the present study we extend the method of Ref. 1 to waveguides with arbitrarily oriented dielectric tensors. We begin by recasting Maxwell's equations as scalar-wave equations for the Cartesian components of the modal fields, with coupling terms based on waveguide geometry and material anisotropy. A perturbative solution that is valid in the limit of small anisotropy and weak guidance is presented, and an expression for the leakage loss is given. A simple general form for the coupling term is derived and is applied to the calculation of the leakage rate for various planar and circular waveguides.

2. DERIVATION OF THE MODAL FIELDS AND THE LOSS

In this section we recast Maxwell's equations for a waveguide of arbitrary anisotropy as a set of coupled scalar equations for the Cartesian components of the modal fields. We then obtain the modal fields to first order and propagation constants to second order in the coupling. The loss is proportional to the imaginary component of the propagation constant. In the following derivation we follow the perturbation method and the notation of Ref. 1 wherever possible.

A. Modal-Field Equations

A general waveguide is drawn schematically in Fig. 1, where the waveguide axis is along z. From Maxwell's equations and the constitutive relations for the fields we write the equations obeyed by the exact vector modal electric fields $\overline{\mathbf{E}}$ as

$$\nabla^2\overline{\mathbf{E}} + k^2\boldsymbol{\epsilon}\cdot\overline{\mathbf{E}} = \nabla(\nabla\cdot\overline{\mathbf{E}}), \tag{1}$$

$$\nabla\cdot(\boldsymbol{\epsilon}\cdot\overline{\mathbf{E}}) = 0, \tag{2}$$

where $k = \omega/c$ is the free-space propagation constant and the magnetic permeability μ has been assumed to take the vacuum value μ_0. For an ideal waveguide oriented along the z axis, the dielectric tensor $\boldsymbol{\epsilon}$ is a function only of the transverse coordinates, i.e., $\boldsymbol{\epsilon} = \boldsymbol{\epsilon}(x, y)$.

The most general possible dielectric tensor $\boldsymbol{\epsilon}'$ for a lossless nongyrotropic medium is symmetric and has six independent elements $\epsilon'_{I,J}$, where $I, J = 1, 2, 3$ and refer to the crystallographic axes. For simplicity we derive the results for the case in which the medium is uniaxial and the optical axis $\hat{3}$ lies in the y–z plane at an angle α to z (we assume a uniform α through the waveguide, contrary to what is done in Ref. 9). Referred to these axes, the dielectric

0740-3232/93/020246-16$05.00

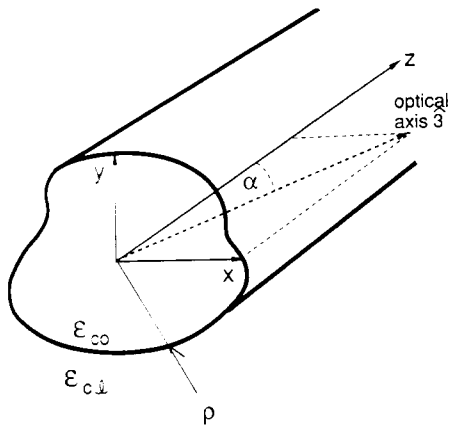

Fig. 1. Waveguide structure is lossless and z invariant. The characteristic transverse dimension is ρ; the dielectric tensor is ϵ_{co} in the core region and ϵ_{ci} in the cladding. For uniaxial media, optical axis $\hat{3}$ lies at an angle α to z in the y–z plane.

tensor ϵ takes the form

$$\epsilon = \begin{bmatrix} \epsilon_{xx} & 0 & 0 \\ 0 & \epsilon_{yy} & \epsilon_{yz} \\ 0 & \epsilon_{yz} & \epsilon_{zz} \end{bmatrix}, \tag{3}$$

where the ϵ_{ij} are given in term of the ϵ'_{IJ} as

$$\begin{aligned} \epsilon_{xx} &= \epsilon'_{11}, \\ \epsilon_{yy} &= \epsilon'_{11}\cos^2\alpha + \epsilon'_{33}\sin^2\alpha, \\ \epsilon_{zz} &= \epsilon'_{11}\sin^2\alpha + \epsilon'_{33}\cos^2\alpha, \\ \epsilon_{yz} &= (\epsilon'_{33} - \epsilon'_{11})\sin\alpha\cos\alpha. \end{aligned} \tag{4}$$

Assume a modal field of the form $\bar{\mathbf{E}} = \bar{\mathbf{e}}(x, y)\exp[i(\beta z - \omega t)]$; Eq. (1) becomes

$$(\nabla_t^2 + k^2\epsilon_{xx} - \beta^2)\bar{e}_x = \frac{\partial}{\partial x}\left(\frac{\partial \bar{e}_x}{\partial x} + \frac{\partial \bar{e}_y}{\partial y} + i\beta\bar{e}_z\right), \tag{5a}$$

$$(\nabla_t^2 + k^2\epsilon_{yy} - \beta^2)\bar{e}_y + k^2\epsilon_{yz}\bar{e}_z = \frac{\partial}{\partial y}\left(\frac{\partial \bar{e}_x}{\partial x} + \frac{\partial \bar{e}_y}{\partial y} + i\beta\bar{e}_z\right), \tag{5b}$$

$$(\nabla_t^2 + k^2\epsilon_{zz} - \beta^2)\bar{e}_z + k^2\epsilon_{yz}\bar{e}_y = i\beta\left(\frac{\partial \bar{e}_x}{\partial x} + \frac{\partial \bar{e}_y}{\partial y} + i\beta\bar{e}_z\right), \tag{5c}$$

and Eq. (2) becomes

$$\frac{\partial}{\partial x}(\epsilon_{xx}\bar{e}_x) + \frac{\partial}{\partial y}(\epsilon_{yy}\bar{e}_y + \epsilon_{yz}\bar{e}_z) + i\beta(\epsilon_{zz}\bar{e}_z + \epsilon_{yz}\bar{e}_y) = 0, \tag{6}$$

where $\nabla_t^2 = \partial^2/\partial x^2 + \partial^2/\partial y^2$.

We can obtain an expression for $\bar{e}_z$ from Eq. (6). To separate to first order the contribution of $\bar{e}_z$ of the off-diagonal elements ϵ_{yz} from that of the waveguide structure, we make the substitution

$$\bar{e}_z = -\frac{\epsilon_{yz}}{\epsilon_{zz}}\bar{e}_y + \bar{e}_z'. \tag{7}$$

With Eqs. (6) and (7) we obtain

$$\bar{e}_z' = -\frac{1}{i\beta}\left(\frac{\epsilon_{xx}}{\epsilon_{zz}}\frac{\partial \bar{e}_x}{\partial x} + \bar{e}_x\frac{\epsilon_{xx}}{\epsilon_{zz}}\frac{\partial}{\partial x}\ln\epsilon_{xx} + \frac{\tilde{\epsilon}_{yy}}{\epsilon_{zz}}\frac{\partial \bar{e}_y}{\partial x} + \bar{e}_y\frac{\tilde{\epsilon}_{yy}}{\epsilon_{zz}}\frac{\partial}{\partial x}\ln\tilde{\epsilon}_{yy}\right), \tag{8}$$

where we have assumed that $\rho\beta\epsilon_{zz} \gg \epsilon_{yx}$, which should hold for all cases of practical interest, and have defined

$$\tilde{\epsilon}_{yy} = \epsilon_{yy} - \frac{\epsilon_{yz}^2}{\epsilon_{zz}} \approx \epsilon_{yy}. \tag{9}$$

Eliminating $\bar{e}_z$ from Eqs. (5a) and (5b) using Eqs. (7) and (8) leads to the coupled equations for the transverse components of the modal electric fields

$$(\nabla_t^2 + k^2\epsilon_{xx} - \beta^2)\bar{e}_x = P_{xx}\bar{e}_x + P_{xy}\bar{e}_y. \tag{10a}$$

$$(\nabla_t^2 + k^2\bar{e}_{yy} - \beta^2)\bar{e}_y = P_{yx}\bar{e}_x + P_{yy}\bar{e}_y. \tag{10b}$$

where

$$P_{xx}\bar{e}_x = \frac{\partial}{\partial x}\left[\left(1 - \frac{\epsilon_{xx}}{\epsilon_{zz}}\right)\frac{\partial \bar{e}_x}{\partial x}\right] - \frac{\partial}{\partial x}\left(\bar{e}_x\frac{\epsilon_{xx}}{\epsilon_{zz}}\frac{\partial}{\partial x}\ln\epsilon_{xx}\right), \tag{11a}$$

$$P_{xy}\bar{e}_y = \frac{\partial}{\partial x}\left[\left(1 - \frac{\tilde{\epsilon}_{yy}}{\epsilon_{zz}}\right)\frac{\partial \bar{e}_y}{\partial y}\right] - \frac{\partial}{\partial x}\left(\bar{e}_x\frac{\tilde{\epsilon}_{yy}}{\epsilon_{zz}}\frac{\partial}{\partial y}\ln\tilde{\epsilon}_{yy}\right) - i\beta\frac{\partial}{\partial x}\left(\frac{\epsilon_{yz}}{\epsilon_{zz}}\bar{e}_y\right), \tag{11b}$$

$$P_{yx}\bar{e}_x = \frac{\partial}{\partial y}\left[\left(1 - \frac{\epsilon_{xx}}{\epsilon_{zz}}\right)\frac{\partial \bar{e}_x}{\partial x}\right] - \frac{\partial}{\partial y}\left(\bar{e}_x\frac{\epsilon_{xx}}{\epsilon_{zz}}\frac{\partial}{\partial x}\ln\epsilon_{xx}\right) + \frac{k^2}{i\beta}\frac{\epsilon_{yz}}{\epsilon_{zz}}\frac{\partial}{\partial x}(\epsilon_{xx}\bar{e}_x), \tag{11c}$$

$$P_{yy}\bar{e}_y = \frac{\partial}{\partial y}\left[\left(1 - \frac{\tilde{\epsilon}_{yy}}{\epsilon_{zz}}\right)\frac{\partial \bar{e}_y}{\partial y}\right] - \frac{\partial}{\partial y}\left(\bar{e}_y\frac{\tilde{\epsilon}_{yy}}{\epsilon_{zz}}\frac{\partial}{\partial y}\ln\tilde{\epsilon}_{yy}\right) - i\beta\frac{\partial}{\partial y}\left(\frac{\epsilon_{yz}}{\epsilon_{zz}}\bar{e}_y\right) + \frac{k^2}{i\beta}\frac{\epsilon_{yz}}{\epsilon_{zz}}\frac{\partial}{\partial y}(\tilde{\epsilon}_{yy}\bar{e}_y). \tag{11d}$$

If $\epsilon_{yz} = 0$, Eqs. (11) reduce to those given in Ref. 1 for waveguides with diagonal dielectric tensors.

If the terms on the right-hand sides of Eqs. (11) vanish, Eqs. (10) become uncoupled scalar-wave equations for the Cartesian components of the modal fields. The solutions of these equations are the well-known linearly polarized (LP) modes that are good approximations for the modes of weakly guiding isotropic waveguides. The second term on the right-hand side (RHS) of each part of Eqs. (11) appears even in isotropic waveguides. In Eqs. (11a) and (11d) these terms represent polarization corrections that are due to the waveguide structure,[11] while in Eqs. (11b) and (11c) they cause polarization coupling in two-dimensional waveguides. The first term on the RHS of each part of Eqs. (11) vanishes in isotropic waveguides and represents polarization coupling that is due to the difference between ϵ_{xx} or ϵ_{yy}—the dielectric constant that the small z component of the modal field would be expected to see—and ϵ_{zz}, the dielectric constant that is actually present in an anisotropic structure. The third term on the RHS of each part of Eqs. (11b)–(11d) and the fourth term of Eq. (11d) are present only when a principal axis of the dielectric tensor

is not aligned with the waveguide axis, and they represent coupling induced by the material anisotropy between the small structural z-polarized component of the predominantly x-polarized mode and the z-polarized component of the predominantly y-polarized mode.

The modal field equations (10) for anisotropic weakly guiding structures can be solved with a pertubation expansion. The uncoupled LP modes are taken as the basis modes, with coupling that is due to the perturbation terms on the RHS's of Eqs. (10). Coupling between modes of the same polarization exists when the $P_{ii}\bar{e}_i$ terms do not vanish, while the $P_{ij}\bar{e}_j$ terms give rise to coupling of orthogonal polarizations. We are interested primarily in calculating the loss that occurs when a guided mode is coupled to degenerate radiation modes. Generally speaking, guided and radiation modes of the same polarization are not degenerate, but if the material is anisotropic, degeneracy between modes of orthogonal polarizations can exist.

In Subsection 2.B we carry out the perturbation expansion to second order, the lowest order in which an imaginary component of the propagation constant can appear. If the coupling is between guided modes, a hybrid guided mode results, as is discussed in Ref. 12. If the coupling is between a guided mode and degenerate modes, the guided mode becomes leaky. Equations (10) can be used to describe both of these phenomena, but in this paper we apply them only to the calculation of leaky modes.

Further discussion of the solutions of Eqs. (10) is facilitated if we assume a specific form for the spatial variation of the elements of the principal dielectric tensor,

$$\epsilon'_{JJ}(x,y) = \epsilon'_{JJ,\mathrm{co}}[1 - 2\Delta_J f_J(x,y)], \qquad J = 1,3, \tag{12a}$$

where $\epsilon'_{JJ,\mathrm{co}}$ is the maximum value of the ϵ'_{JJ} component, $2\Delta_J\epsilon'_{JJ,\mathrm{co}}$ is the difference between the dielectric tensor component in the core and the cladding, and Δ_J is known as the profile height. Functions $f_J(x,y)$ describe the spatial variation of the dielectric tensor components, normalized to vary between 0 and 1. By assuming this form, we have restricted the analysis to systems in which the orientation of the principal axes does not depend on the transverse coordinates. The dielectric tensor components ϵ_{xx} and ϵ_{yy} are related to ϵ'_{JJ} through the expressions in Eqs. (4) and hence can be written in the same form as Eq. (12a). In this way the profile heights for the transverse polarizations, Δx and Δy, are introduced. It is convenient to characterize the anisotropy by the quantities δ_{IJ}, defined by

$$\delta_{IJ}(x,y) = \frac{1}{2}\left[1 - \frac{\epsilon'_{II}(x,y)}{\epsilon'_{JJ}(x,y)}\right], \tag{12b}$$

and to use the usual definition of the normalized frequencies $V_i = \rho k n_{i,\mathrm{co}}(2\Delta_i)^{1/2}$, where $i = x, y$ and $n_i = \epsilon_{ii}^{1/2}$ is the refractive index.

Note from the definition of normalized frequency in Table 1 that $\rho\beta \propto \Delta^{1/2}$ for fixed V and $\rho\partial/\partial x$ is of order unity; it is clear that, for weakly guiding ($\Delta \ll 1$) and weakly anisotropic ($\delta \ll 1$) waveguides, the first two terms on the RHS's of Eqs. (11b) and (11c) are small. Thus when $\epsilon_{yz} = 0$, a solution correct to first order in Δ and δ is generally valid. When $\epsilon_{yz} \neq 0$ the third terms on the RHS's of Eqs. (11b) and (11c) are of order $\delta\Delta^{-1/2}$; the terms are small when $\delta \sim \Delta$ but can be large when $\delta \gg \Delta$. However, we will show in Subsection 2.C that these coupling terms are actually of order $\Delta^{1/2}$ and thus can be regarded as perturbations as long as $\Delta, \delta \ll 1$.

The zeroth-order solutions, $e^{(0)}_{(x)x}$ and $e^{(0)}_{(y)y}$, obtained from the homogeneous forms of Eqs. (10), are the familiar linearly polarized modes. We can then construct modal-field solutions to the coupled-field equations (10) in such a way that they are either purely x polarized or y polarized to lowest order. We assume that a predominantly i-polarized mode, written as $\mathbf{e}_{(i)}$, and its propagation constant $\beta_{(i)}$ can be expanded as power series in the small quantities Δ and δ (which are treated as being of the same order):

$$\mathbf{e}_{(i)} = (e^{(0)}_{(i)i} + e^{(1)}_{(i)i} + e^{(2)}_{(i)i} + \ldots)\mathbf{i} + (e^{(1)}_{(i)j} + e^{(2)}_{(i)j} + \ldots)\mathbf{j}, \tag{13a}$$

$$\beta_{(i)} = \beta_{(i)0} + \beta_{(i)1} + \beta_{(i)2} + \ldots. \tag{13b}$$

We can evaluate the series given in Eqs. (13) by substituting them into Eqs. (10) and equating like powers of the perturbation, which gives the approximate equations for a predominantly i-polarized mode:

$$(\nabla_t^2 + k^2\epsilon_{ii} - \beta^2_{(i)0})e^{(0)}_{(i)i} = 0, \tag{14a}$$

$$(\nabla_t^2 + k^2\epsilon_{jj} - \beta^2_{(i)0})e^{(1)}_{(i)j} = P_{ij}e^{(0)}_{(i)i}, \tag{14b}$$

$$(\nabla_t^2 + k^2\epsilon_{ii} - \beta^2_{(i)0})e^{(1)}_{(i)i} = 2\beta_{(i)0}\beta_{(i)1}e^{(0)}_{(i)i} + P_{ii}e^{(0)}_{(i)i}, \tag{14c}$$

$$(\nabla_t^2 + k^2\epsilon_{ii} - \beta^2_{(i)0})e^{(2)}_{(i)i} = (2\beta_{(i)0}\beta_{(i)2} + \beta^2_{(i)1})e^{(0)}_{(i)i} + 2\beta_{(i)0}\beta_{(i)1}e^{(1)}_{(i)i} + P_{ii}e^{(1)}_{(i)i} + P_{ij}e^{(1)}_{(i)j}. \tag{14d}$$

Table 1. Waveguide Parameters

Parameters	Polarization x	Polarization y		
Dielectric Constant	$\epsilon_{xx} = \epsilon_{11}'$	$\epsilon_{yy} = \epsilon_{11}'\sin^2\alpha + \epsilon_{33}'\cos^2\alpha$		
Profile	$n_x(x,y) = (\epsilon_{xx})^{1/2}$	$n_y(x,y) = (\epsilon_{yy})^{1/2}$		
Profile Height	$\Delta_x = \Delta_1$	$\Delta_y = \Delta_1\cos^2\alpha + \Delta_3\sin^2\alpha$		
Normalized Frequency[a]	$V_x = \rho k n_{x,\mathrm{co}}(2\Delta_x)^{1/2}$	$V_y = \rho k n_{y,\mathrm{co}}(2\Delta_y)^{1/2}$		
Principal Dielectric Constant			$\epsilon_{II}'(x,y) = \epsilon'_{II,\mathrm{co}}[1 - 2\Delta_I f_I(x,y)]$	$I = 1,3$
Principal Profile Height			$\Delta_I = (1 - \epsilon'_{II,\mathrm{cl}}/\epsilon'_{II,\mathrm{co}})/2$	$I = 1,3$
Anisotropy			$\delta_{IJ} = (1 - \epsilon'_{II}/\epsilon'_{JJ})/2,$	$I, J = 1,3$

[a] $k = 2\pi/\lambda$; ρ is the dimension of the core region.

Table 2. Modal Parameters[a]

Parameters	Polarization	
	y (Guided)	x (Radiation)
Propagation constant	$\beta_{(y)}$	$\beta_{(x)}$
Core parameter	$U_y = \rho(k^2\epsilon_{yy,\mathrm{co}} - \beta_{(y)}^2)^{1/2}$	$U_x = \rho(k^2\epsilon_{xx,\mathrm{co}} - \beta_{(x)}^2)^{1/2}$
Cladding parameter	$W_y = \rho(\beta_{(y)}^2 - k^2\epsilon_{yy,\mathrm{cl}})^{1/2}$	$Q_x = \rho(k^2\epsilon_{xx,\mathrm{cl}} - \beta_{(x)}^2)^{1/2}$
Normalization constant	$\langle e_{(y)y}^{(0)\,2}\rangle$	$\langle e_{(x)x}^{*(0)}(Q_x')e_{(x)x}^{(0)}(Q_x)\rangle = N_q\delta(Q_x - Q_x')$

[a] $V_y^2 = U_y^2 + W_y^2$; $U_x^2 + Q_x^2 = V_x^2$; $U_x^2 = V_y^2\delta_{31,\mathrm{co}}/\Delta_y \sin^2\alpha + U_y^2$, when $\beta(y) = \beta(x)$.

Modes constructed by this method are orthogonal to each other to first order in Δ and δ. For higher-order perturbations $\beta_{(i)}$ is complex, Eqs. (14) are not Hermitian operator equations, and the set of eigenmodes $\mathbf{e}_{(i)}$ is not mutually orthogonal but has a biorthogonal relationship with the modes of the transpose equations of Eqs. (14).[13]

B. Solution of the Approximate Field Equations

We are interested primarily in calculating the leakage loss resulting from the anisotropy, and so we must obtain the imaginary part of the propagation constant. If we assume an i-polarized zeroth-order mode, the first-order correction to the propagation constant $\beta_{(i)1}$ is the expectation value of the coupling for the zeroth-order mode and can be obtained from Eqs. (14a) and (14c) with the use of standard perturbation theory. It can be shown that $\beta_{(i)1}$ is real. We then must obtain the second-order correction to find the loss. Multiplying Eq. (14d) by $e_{(i)i}^{(0)}$ and using the orthogonality of $e_{(i)i}^{(1)}$ and $e_{(i)i}^{(2)}$ to $e_{(i)i}^{(0)}$, we arrive at[1]

$$\beta_{(i)2} = -\frac{1}{2\beta_{(i)0}}\left[\beta_{(i)1}^2 + \frac{\langle e_{(i)i}^{(0)}P_{ii}e_{(i)i}^{(1)}\rangle}{\langle e_{(i)i}^{(0)2}\rangle} + \frac{\langle e_{(i)i}^{(0)}P_{ij}e_{(i)j}^{(1)}\rangle}{\langle e_{(i)i}^{(0)2}\rangle}\right], \quad (15)$$

where we use the symbol $\langle g\rangle$ to denote an integral of $g(x, y)$ over the x–y plane. As is discussed in Section 1 and in Appendix A, only coupling to degenerate radiation modes of the orthogonal polarization leads to loss, so that only the third term in Eq. (15) contributes to the imaginary part of $\beta_{(i)}$. An integral expression for $e_{(i)j}^{(1)}$, first given in Ref. 1, is discussed in the context of the present analysis in Appendix A. It is shown there that using the integral expression for $e_{(i)j}^{(1)}$, given by Eq. (A1.4), in Eq. (15) leads to

$$\beta_{(i)2}^{\mathrm{im}} = \begin{cases} \dfrac{\pi\rho^2}{2\beta_{(i)0}}\dfrac{|\langle e_{(i)i}^{(0)}P_{ij}e_{(i)j}^{(0)}\rangle|^2}{2N_qQ_j\langle e_{(i)i}^{(0)2}\rangle}, & \beta_{(i)0} < \beta_{\mathrm{th}} \\ 0 & \beta_{(i)0} > \beta_{\mathrm{th}} \end{cases}, \quad (16)$$

where $\beta_{\mathrm{th}} = kn_{j,\mathrm{cl}}$, $e_{(j)j}^{(0)}(Q_j)$ is the j-polarized LP radiation mode satisfying $\beta_{(j)0,q} = \beta_{(i)0}$, and N_q and Q_j, defined in Table 2, are the normalization constant and the cladding parameter of the radiation mode, respectively. The limits to the validity of this expansion are discussed in Subsection 2.C after a simplified form of the coupling coefficient is derived.

C. Simplification of the Coupling Terms $\langle e_{(i)i}^{(0)}P_{ij}e_{(j)j}^{(0)}\rangle$

The expressions for the coupling terms that are necessary for the evaluation of Eq. (16), given by Eqs. (11), are obviously complicated. In this section we develop relations that will both simplify the calculation and yield physical insight into the leaky modes. The simplified coupling coefficients illustrate more clearly the dependence of the leakage rate on the material anisotropy δ_{31}, the profile height Δ, and the angle α between the optical and the waveguide axes, without evaluation of the coupling integral or detailed information about LP modes. The transformed coupling coefficient, which involves the modal fields only in the region of the spatially varying refractive index rather than in all space and does not require the spatial derivatives of the modal fields, often yields more accurate results than does direct application of Eq. (16) when approximations to the modal fields are used.

We assume that the dielectric tensors of the waveguide media are of the form given in Eqs. (3) and (4); that the orientation of the principal axes is the same throughout the structure; and, in addition, that $\epsilon_{yy,\mathrm{cl}} < \epsilon_{xx,\mathrm{cl}}$, i.e., that the media are negative uniaxial. Since the x-polarized modes are the slow modes, only the y-polarized modes exhibit leakage. Thus in evaluating Eq. (16) we take $i = y$ and $j = x$. Any of the expressions derived under these assumptions can be applied to positive uniaxial media by interchanging the coordinates x and y.

Under these assumptions, leaky modes do not exist when $\alpha = 0$. Anisotropy in the x–y plane emerges when $\alpha \neq 0$, and leakage begins when α exceeds a threshold value α_{th}, as we discuss in Section 3. In planar waveguides the coupling that leads to the leakage is attributable exclusively to the third terms on the RHS's of Eqs. (11b) and (11c). In two-dimensional guides all three terms on the RHS's of Eqs. (11b) and (11c) are nonvanishing, but the third terms generally dominate, as is discussed in Section 4. Therefore we focus our attention on these dominant terms and present some results for the other terms in later sections. Retaining only the most important terms in Eq. (11c), we have

$$\langle e_{(y)y}^{(0)}P_{yx}e_{(x)x}^{(0)}\rangle = \frac{k^2}{i\beta}\left\langle e_{(y)y}^{(0)}\epsilon_{yz}\frac{\partial e_{(x)x}^{(0)}}{\partial x}\right\rangle. \quad (17)$$

As we know, $e_{(y)y}^{(0)}$ and $e_{(x)x}^{(0)}$ satisfy the homogeneous forms of Eqs. (10). For convenience we list them again as follows:

$$(\nabla_t^2 + k^2\epsilon_{yy} - \beta_{(y)0}^2)e_{(y)y}^{(0)} = 0, \quad (18a)$$

$$(\nabla_t^2 + k^2\epsilon_{xx} - \beta_{(x)0}^2)e_{(x)x}^{(0)} = 0. \quad (18b)$$

For the radiation mode that is degenerate with the guided mode, i.e., $\beta_{(y)0} = \beta_{(x)0}$, it can be readily derived from Eq. (18b) that

$$(\nabla_t^2 + k^2\epsilon_{xx} - \beta_{(y)0}^2)\frac{\partial e_{(x)x}^{(0)}}{\partial x} = -k^2e_{(x)x}^{(0)}\frac{\partial\epsilon_{xx}}{\partial x}. \quad (19)$$

Multiplying Eq. (19) by $e_{(y)y}^{(0)}$ and Eq. (18a) by $e_{(x)x}^{(0)}$, subtracting, and integrating over the x–y plane, we obtain

$$\left\langle (\epsilon_{xx} - \epsilon_{yy}) e^{(0)}_{(y)y} \frac{\partial e^{(0)}_{(x)x}}{\partial x} \right\rangle = -\left\langle \frac{\partial \epsilon_{xx}}{\partial x} e^{(0)}_{(y)y} e^{(0)}_{(x)x} \right\rangle. \quad (20)$$

Making use of Eq. (20) and a relation

$$(\epsilon_{xx} - \epsilon_{yy}) = (\epsilon'_{11} - \epsilon'_{33}) \sin^2 \alpha \approx -\epsilon_{yz} \tan \alpha \quad (21)$$

derived from Eqs. (4), we find that

$$\left\langle e^{(0)}_{(y)y} \epsilon_{yz} \frac{\partial e^{(0)}_{(x)x}}{\partial x} \right\rangle = \cot \alpha \left\langle \frac{\partial \epsilon_{xx}}{\partial x} e^{(0)}_{(y)y} e^{(0)}_{(x)x} \right\rangle. \quad (22)$$

Combining Eqs. (12a), (16), (17), and (22), we obtain the relatively simple form for the imaginary part of the propagation constant:

$$\beta^{\mathrm{im}}_{(y)2} = \begin{cases} \beta_{(y)0} \dfrac{\pi \rho^2 \Delta_x \cot^2 \alpha}{\langle e^{(0)2}_{(y)y} \rangle} \dfrac{\left| \left\langle \dfrac{\partial f_x}{\partial x} e^{(0)}_{(y)y} e^{(0)}_{(x)x} \right\rangle \right|^2}{N_q Q_x}, & \beta_{(y)0} < \beta_{\mathrm{th}} \\ 0, & \beta_{(y)0} > \beta_{\mathrm{th}} \end{cases} \quad (23)$$

where $e^{(0)}_{(x)x}$ is the radiation mode that is degenerate with $e^{(0)}_{(y)y}$ and β_{th} is given by Eq. (A7), with $j = x$. Equation (23) is derived under the assumption that the medium is uniaxial.

With Eq. (23) it can be shown that the perturbation expansion in Eqs. (13) is valid, in the sense that $|\rho^2 \beta_{(y)0} \beta_{(y)1}| \ll 1$ and $|\beta_{(y)2}| \ll |\beta_{(y)1}|$, where $\beta_{(y)1}$ is the first-order correction to $\beta_{(y)}$ and the first-order corrections to the modal fields are much smaller than the LP basis modes, as long as the waveguide is weakly guiding and the media are weakly anisotropic, i.e., as long as $\Delta_1, \Delta_3 \ll 1$ and $\delta_{31} \ll 1$. Many of the waveguides used in integrated optics are strongly asymmetric, violating the weak-guidance condition at one interface. It is shown in Section 5 that the perturbative approach is still adequate for such waveguides.

3. SYMMETRIC STEP-PROFILE PLANAR WAVEGUIDE

Despite the existence of exact solutions for the step-profile planar waveguide,[2] it is useful to apply the present approximation technique to this case, both as a test of the method and to develop simple closed-form expressions for the dependence of the loss on various waveguide parameters. The results that are obtained for the step-profile planar guide are prototypical of those that are obtained for more complicated structures in Sections 4 and 5.

We assume a waveguide of the form shown in Fig. 2, with a step profile $\partial f/\partial x = \delta(x + \rho) - \delta(x - \rho)$, where ρ is the half-thickness of the guiding layer. Since $\partial f/\partial x$ is odd, the imaginary part of the propagation constant given by Eq. (23) is nonzero only when the product of the y-polarized zeroth-order mode $e^{(0)}_{(y)y}$ and the degenerate x-polarized radiation mode $e^{(0)}_{(x)x}$ is odd. If $e^{(0)}_{(y)y}$ is even, the expressions for the LP modes, $e^{(0)}_{(y)y}$ and $e^{(0)}_{(x)x}$, given in Eqs. (A2.1) and (A2.2), can be used in Eq. (23) to find

$$\beta^{\mathrm{im}}_{(y)2} = [4\beta_{(y)0} \Delta_x^2 \cot^2 \alpha] \times \left(\frac{U_y^2/V_y^2}{1 + 1/W_y} \right) \left\{ \frac{\sin^2 U_x}{Q_x [1 + (V_x^2/Q_x^2) \cos^2 U_x]} \right\}, \quad (24)$$

where Q_x, U_x, U_y, and W_y are modal parameters that are defined in Table 2, and V_y is the normalized frequency for the y polarization that is defined in Table 1. Note that this expression contains three factors, the first of which is independent of the modal parameters, the second of which depends only on the parameters of the guided mode, and the third of which depends only on the parameters of the radiation mode. It will be seen that similar forms hold for the more complex waveguides that are discussed in Section 4. For odd $e^{(0)}_{(y)y}$, the imaginary part of the propagation constant can be obtained from Eq. (24) by interchanging $\sin U_x$ and $\cos U_x$.

Several basic features of the loss can be seen in Fig. 3, where the power-loss coefficient, $2\beta^{\mathrm{im}}$, in decibels per centimeter, is plotted against α for a waveguide with the same parameters as those given in Fig. 6 of Ref. 2. The loss vanishes for α that is smaller than a threshold angle α_{th}, rises steeply to a maximum, and then rolls off slowly with a series of similarly spaced minima. Quantitative description and qualitative understanding of these phenomena are facilitated by rewriting the expression for the loss as a product of a smooth envelope function g (shown by the dashed curve in Fig. 3) and a positive definite oscillatory function h, which is of order unity except in special cases to be discussed later in this section. Thus $\beta^{\mathrm{im}}_{(y)2} = gh$, where g and h are given by

$$g = \beta_{(y)0} \begin{cases} 4\Delta_x^2 \cos^2 \alpha \dfrac{W_y U_y^2}{V_y^2 (1 + W_y)} \dfrac{Q_x}{U_x^2}, & \alpha > \alpha_{\mathrm{th}} \\ 0, & \alpha < \alpha_{\mathrm{th}} \end{cases} \quad (25)$$

$$h = \frac{\sin^2 U_x}{[(Q_x^2/U_x^2) \sin^2 U_x + \cos^2 U_x]}. \quad (26)$$

The basic features of the envelope function are the threshold angle below which the loss vanishes, α_{th}; the maximum value of the loss g_p, which occurs at an angle α_p; and the slow decrease with increasing α up to $\alpha = \pi/2$, where the envelope vanishes. For angles smaller than α_{th}, $\beta_{(y)0}$, the propagation constant of the guided LP mode $e^{(0)}_{(y)y}$, is larger than β_{th}, so that no x-polarized radiation modes are degenerate with the y-polarized guided mode, which then propagates without leakage. When $\alpha > \alpha_{\mathrm{th}}$, $\beta_{(y)0} > \beta_{\mathrm{th}}$, degenerate radiation modes exist, and the y-polarized mode is leaky. Within the range of angles

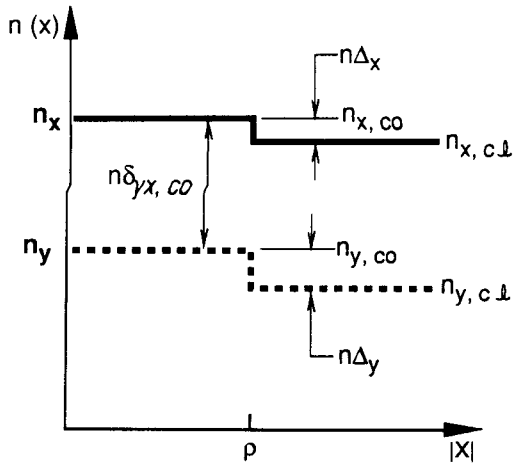

Fig. 2. Example of a symmetric step-profile planar waveguide and definitions of the refractive indices.

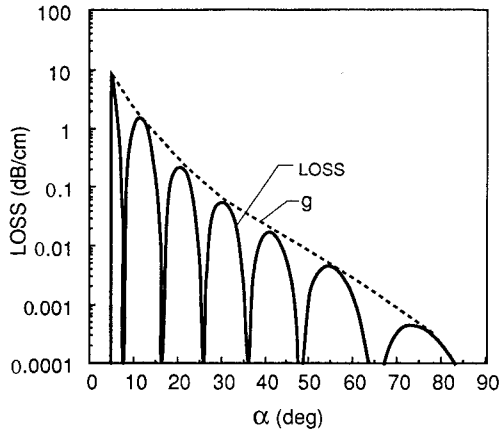

Fig. 3. Loss coefficients for the lowest-order mode of a symmetric step-profile planar waveguide, in decibels per centimeter, as a function of α (solid curve), calculated with Eq. (24). The dashed curve is the envelope function defined in Eq. (25). The half-thickness of the guiding layer is $\rho = 3$ μm, the vacuum wavelength $\lambda = 0.6328$ μm, the refractive indices are $n_{1,co} = 2.281$ and $n_{3,co} = 2.174$, and the profile heights are $\Delta_1 = 0.0005$ and $\Delta_3 = 0.002$. The parameters of the refractive indices are chosen to be the same as those used in Fig. 6 of Ref. 2.

where degenerate radiation modes exist, the magnitude of the leakage depends, according to Eqs. (16) and (17), on the square of the product of ϵ_{yz} and an overlap integral between the degenerate modes. At large angles the leakage is small because of the sin 2α dependence of ϵ_{yz}, while for small angles the loss peak results from a trade-off between the increase in ϵ_{yz} and the rapid decrease in overlap integral with α. The overlap is large for small α because the waveguide is nearly isotropic; and, in an isotropic waveguide, degeneracy between a guided and a radiation mode can occur only as the guided mode approaches cutoff. For fixed Δ_x, g decreases as V_y increases. When the profile height is much smaller than the anisotropy, g is proportional to $\Delta_x^2\Delta_y^{1/2}/\delta_{31}^{1/2}$ for fixed V_y.

Using the definitions of the modal parameters given in Table 2, we can obtain the threshold angle α_{th} from the expression for β_{th} in Eq. (A7) [taking $j = x$ in Eq. (A7)]. We find that

$$\sin^2 \alpha_{th} = \left(\frac{\Delta_y}{|\delta_{31,cl}|}\frac{W_y^2}{V_y^2}\right)_{\alpha=\alpha_{th}}, \tag{27}$$

where $(W_y/V_y)^2$ is only a function of V_y and is denoted conventionally as $b(Vy)$.[14] Both $\delta_{13,cl}$ and $\Delta_y/(V_y)^2$ are independent of α, but V_y and thus W_y are functions of α. If Δ_1 and Δ_3 are equal, V_y is independent of α, as is the RHS of Eq. (27); therefore α_{th} can be expressed in closed form. Otherwise, both sides of Eq. (27) are functions of α_{th}, and α_{th} can be obtained only numerically. As $b(V_y) \leq 1$, α_{th} is small when the profile height is small compared with the anisotropy but can approach $\pi/2$ when Δ_y approaches $\delta_{31,cl}$.

α_p can be derived if we set the derivative $\partial g/\partial\alpha = 0$. Assuming that $(\alpha_p - \alpha_{th}) \ll \alpha_{th}$ and $\Delta_y \ll \delta_{31,cl}$, we get

$$\frac{\alpha_p}{\alpha_{th}} = \left\{1 + \frac{-(3 + 2\kappa) + [(3 + 2\kappa)^2 + 40\kappa]^{1/2}}{20\kappa}\right\}_{\alpha=\alpha_{th}}, \tag{28a}$$

where

$$\kappa = \frac{\Delta_y}{\Delta_x}b. \tag{28b}$$

The second term in Eq. (28a) can be approximated reasonably well by $1/3(1 + \kappa)$. Using this approximation, we obtain the maximum value of the envelope function by substituting α_p into the expression for g given in Eq. (25), which results in

$$g_p = \gamma\beta_{(y)0}\Delta_x\delta_{31,cl}, \tag{29a}$$

where

$$\gamma = \left[\frac{9\sqrt{6}(1 - b)(1 + \kappa)^{5/2}}{(V_y\sqrt{b} + 1)(4 + 3\kappa)^2(3 + 5\kappa)}\right]_{\alpha=\alpha_{th}}. \tag{29b}$$

γ is 0.46 at $V_y = 0$, decays as V_y increases, and can be approximated by $0.785/V_y^3$ when $V_y \gg 1$ and $\Delta_y = \Delta_x$. The last two factors in Eq. (29a) show a linear increase with the anisotropy and the profile height when V is fixed. Comparing the expression for g_p with that for g obtained from Eq. (25), and using the expressions for U_x and Q_x given in Table 2, we find that as the anisotropy increases, the peak of the envelope increases, but the envelope decreases at large α, i.e., the loss becomes peaked in the small α region.

The oscillatory function h [Eq. (26)] is related to the properties of the radiation mode that is degenerate with the guided mode. As α increases, the denominator in the expression for h is generally of order unity, so that the nearly periodic minima in the leakage are due primarily to the $\sin^2 U_x$ factor in the numerator. These minima can be understood either in a ray picture, where the loss vanishes when the radiation transmitted on successive reflections interferes destructively,[2] or in a modal picture, where the loss vanishes according to the transformed overlap integral [Eq. (23)] when the magnitude of the x-polarized radiation mode at the core–cladding interface vanishes. The condition for the occurrence of a minimum is $U_x = m\pi$, where m is an integer. While these minima are equally spaced in U_x, they are not in general equally spaced in α, because of the nonlinear dependence of U_x on α (see Table 2). If $\Delta_y \ll \delta_{31,cl}$, we can use the approximate expression for U_x in Table 2 to obtain the angular separations between the minima as

$$\alpha_m - \alpha_{m-1} = c\{m[1 - c^2(m - 1)^2]^{1/2} - (m - 1)[1 - c^2m^2]^{1/2}\}, \tag{30a}$$

where c is independent of α and is given by

$$c = \frac{\pi}{V_y}\left(\frac{\Delta_y}{\delta_{31,\omega}}\right)^{1/2}. \tag{30b}$$

Noting that $V_y/\Delta_y^{1/2} \sim \rho\beta_{(y)0}$, we see that the spacing is independent of Δ_y if the thickness of the waveguide is fixed.

Exact solutions for the modal fields and a transcendental equation for β that is solved numerically are presented in Ref. 2. It can be shown that, to first order in Δ and δ, the exact solution for β^{im} deduced from Eq. (26) of Ref. 2 and the perturbative result obtained here are identical [except when the degenerate radiation mode is just above the cutoff of an odd guided mode, i.e., when $V_x \approx (1/2 + m)\pi$]. The approximate values for the loss that are presented in Fig. 3 are indistinguishable on the scale of the graph from the results obtained from the exact analysis of Ref. 2.

Figure 4 shows the losses of two waveguides with the same V_y and δ_{31} but with different Δ (for simplicity, we

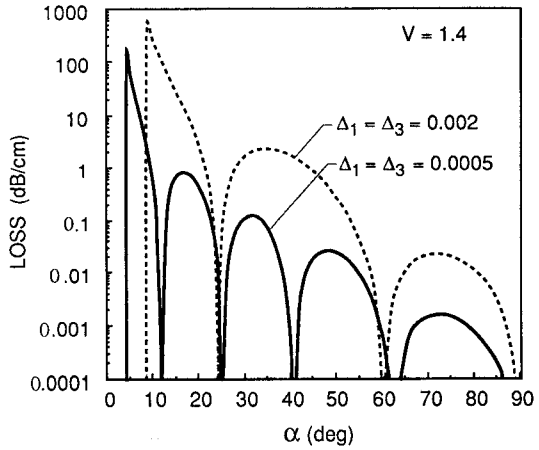

Fig. 4. Loss of the lowest-order leaky modes for two symmetric step-profile planar waveguides with the same normalized frequencies $V = 1.4$. The refractive indices in the film for both waveguides are chosen as $n_{1,co} = 2.281$ and $n_{3,co} = 2.174$. The profile heights, assumed to be the same for ordinary and extraordinary polarizations but different for the two waveguides, are 0.0005 for the solid curve and 0.002 for the dashed curve. The wavelength is $\lambda = 0.6328$ μm.

choose $\Delta_1 = \Delta_3$; therefore $\Delta_x = \Delta_y = \Delta$ and $V_y = V_x = V$), and $\Delta \ll \delta$. For waveguides with fixed V and δ_{31}, Eq. (27) indicates that the threshold angle α_{th} is proportional to the square root of Δ, Eq. (29a) shows that the peak of the envelope increases linearly with Δ, and it can be deduced from Eq. (25) that the envelope function g is proportional to $\Delta^{5/2}$, a result that is consistent with the results shown in Fig. 4.

While estimates of β^{im} based on the envelope function g are generally valid for $\alpha > \alpha_{th}$, in the vicinity of the first loss peak the oscillatory function h can have a significant effect on the magnitude of the loss in certain cases. If a zero of h occurs near α_{th}, the peak of the loss is reduced and the location of the peak shifts slightly. If $Q_x \to 0$ and $V_x \to (m + 1/2)\pi$, it can be seen from Eq. (26) that $h \to \infty$. The calculated loss then diverges, and the perturbation method clearly is no longer valid. This result is consistent with the exact results of Ref. 2, which show that in this limit $\rho\beta^{im}$ is of order unity, so that the loss is extremely large and the perturbation method can be expected to break down. In the context of the present analysis these conditions correspond to the degeneracy of the guided mode with a radiation mode that is just at cutoff.

Figure 5 illustrates the losses of two waveguides with the same ρ and δ_{31} but different Δ (again, $\Delta_x = \Delta_y = \Delta$, and $V_y = V_x = V$) and therefore different V. From Fig. 5 we can see that the losses for $\Delta = 0.002$ are generally larger than those for $\Delta = 0.0005$ except in the vicinity of the first loss peak, and the minima of the two losses occur at the same angle. The magnitude of the loss for $\alpha \neq \alpha_{th}$ is dominated by the Δ^2 scaling of g that can be seen from Eq. (25), and the positions of the minima follow from Eq. (30). The threshold angle α_{th}, given by Eq. (27), varies only with W_y for waveguides with fixed ρ, so that the smaller α_{th} for the waveguide with smaller Δ is expected. For $\alpha = \alpha_{th}$, the magnitude of the loss can be calculated by using the limiting form of $h \approx \tan^2 V$ obtained from Eq. (26) with $Q_x \ll 1$. In this limit, $gh \sim \gamma V^2 \tan^2 V$ for fixed ρ, so that the smaller peak loss for the waveguide with larger Δ can be seen from $\gamma V^2 \tan^2 V = 7.04$ for $\Delta = 0.002$ and $\gamma V^2 \tan^2 V = 0.012$ for $\Delta = 0.0005$. For large V the limiting form $\gamma V^2 \to 0.785/V$ is convenient.

4. OTHER EXAMPLES OF WEAKLY GUIDING WAVEGUIDES

A. Asymmetric Step-Profile Planar Waveguides

Most waveguides that are used in practical applications are strongly asymmetric. In this section we consider the behavior of asymmetric waveguides but keep the assumption of weak guidance at both interfaces. In Section 5 we consider the extension to the case of one weakly guiding and one strongly guiding interface.

The form of the step-profile asymmetric planar waveguide considered in this section is illustrated in Fig. 6, where it is assumed that $n_{x,cl1} < n_{x,cl2}$ and $\partial f/\partial x = (\Delta_{x2}/\Delta_{x1})\delta(x + \rho) - \delta(x)$, with ρ the thickness of the waveguide. If $kn_{x,cl1} < \beta_{(y)0} < kn_{x,cl2}$ (which is usually the case for small α, especially when α is near the threshold angle),

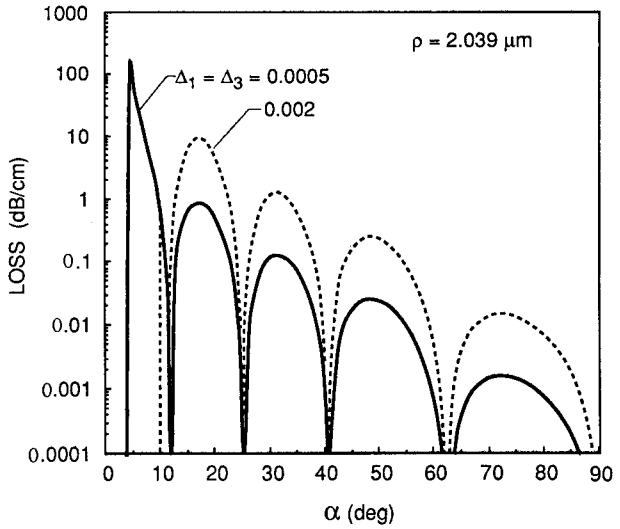

Fig. 5. Loss coefficients of the lowest-order leaky modes for two symmetric step-profile planar waveguides with the same half-thickness $\rho = 2.039$ μm. The refractive indices of the waveguides (solid and dashed curves) are the same as those of the waveguides (solid and dashed curves) in Fig. 4.

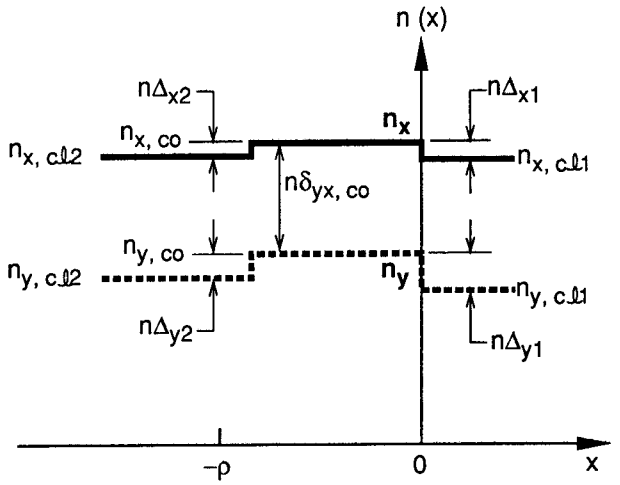

Fig. 6. Step-index profiles for an asymmetric planar waveguide with thickness ρ.

and if we use the expressions for LP modes $e^{(0)}_{(y)y}$ and $e^{(0)}_{(x)x}$ given in Eqs. (B6) and (B9) and their normalization constants $\langle e^{(0)2}_{(y)y}\rangle$ and N_{q2}, given by Eqs. (B7) and (B12), respectively, Eq. (23) for the loss becomes

$$\beta^{\mathrm{im}}_{(y)2} = \chi \frac{[(\Delta_{y2}/\Delta_{y1})^{1/2}U_x/V_{x2} - (\Delta_{x2}/\Delta_{x1})^{1/2}\sin(U_x - \phi_{x1})]^2}{Q_{x2}[1 + V_{x2}^2/Q_{x2}^2\cos^2(U_x - \phi_{x1})]}, \tag{31a}$$

where

$$\chi = (4\beta_{(y)0}\Delta_{x1}\Delta_{x2}\cot^2\alpha)\left[\frac{U_y^2/V_{y2}^2}{1 + (1/W_{y1}) + (1/W_{y2})}\right]. \tag{31b}$$

Notice that, following the notation of Refs. 15 and 16, the characteristic dimension ρ, used in the normalized frequency V, is the full thickness for asymmetric waveguides and the half-thickness for symmetric waveguides.

If $\beta_{(y)0} < kn_{x,\mathrm{cl1}}$, the radiation modes propagate in both cladding regions and for each propagation constant two kinds of radiation modes exist, so that Eq. (23) becomes a sum of two terms. Using Eq. (B13) for the two types of radiation mode, we obtain

$$\beta^{\mathrm{im}}_{(y)2} = \chi \sum_{m=1,2} \frac{(\{(\Delta_{y2}\Delta_{x1})/[\Delta_{y1}\Delta_{x2}(1 + F_m^2)]\}^{1/2} - (\Delta_{x2}/\Delta_{x1})^{1/2}\cos(U_x - \phi_{fm}))^2}{Q_{x2}\{1 + (V_{x2}^2)/(Q_{x2}^2)\sin^2(U_x - \phi_{fm}) + (Q_{x1}/Q_{x2})[1 + (V_{x1}^2/Q_{x1}^2)(F_m^2/1 + F_m^2)]\}}, \tag{32}$$

where the F_m, parameters in the expressions for the radiation modal field, are given by Eq. (B15) and $\phi_{fm} = \cos^{-1}[1/(1 + F_m^2)^{1/2}]$.

While the form of the expressions for the loss for an asymmetric waveguide, Eqs. (31a) and (32), is substantially more complicated than that for a symmetric waveguide, Eq. (24), the essential behaviors of these waveguides are similar. Figure 7 shows the loss for an asymmetric waveguide whose parameters are the same as those of the symmetric waveguides shown in Fig. 5, except that $\Delta_{y1} = \Delta_{x1} = 0.002$ and $\Delta_{y2} = \Delta_{x2} = 0.0005$ (again, $\Delta_1 = \Delta_3$, and thus $\Delta_y = \Delta_x$). We can see that, except in the vicinity of α_{th}, the envelope of the loss for the asymmetric guide falls between the envelopes of the symmetric waveguides, and the oscillations of the loss are weaker for the asymmetric waveguide. The behavior of the envelopes could be anticipated from the first factors in Eqs. (31a) and (32), χ, which contain the product $\Delta_{x1}\Delta_{x2}$. It can be shown that $(\Delta_{y2}/\Delta_{y1})^{1/2}U_x/V_{x2} > (\Delta_{x2}/\Delta_{x1})^{1/2}$ is generally true when $kn_{x,\mathrm{cl1}} < \beta_{(y)0} < kn_{x,\mathrm{cl2}}$. When $\beta_{(y)0} < kn_{x,\mathrm{cl1}}$, the magnitude of one of the F_m [which could be either F_1 or F_2 depending on the sign of $\sin(2U_x)$], is smaller than 1/2, the loss from the coupling to the mode with the smaller F_m dominates, and $(\Delta_{y2}\Delta_{y1})(\Delta_{x1}/\Delta_{x/2})^2 > 1 + F_m^2$ for this smaller F_m. Therefore the oscillatory function represented by the third factor in Eqs. (31a) and (32) has no zeros. The divergence in the calculated loss noted for the symmetric waveguide when the guided mode is degenerate with a near-cutoff radiation mode is also observed in the asymmetric waveguide, and it occurs when $V_{x2} = \cos^{-1}(\Delta_{x2}/\Delta_{x1})^{1/2} + (1/2 + m)\pi$, which is again the cutoff condition for the mth guided mode.

B. Step-Profile Circular Fiber

Analytical solutions for the modes of anisotropic fibers exist only when the optical and the fiber axes are parallel.[17] However, with weak-guidance and weak-anisotropy assumptions, approximate solutions are possible. Here we consider step-index fibers, as they yield simple results and are prototypical of other index profiles. Such step-profile anisotropic fibers can be obtained experimentally, for example, by growth of organic-crystal cores in glass capillaries[18] or by diffusion of claddings in lithium niobate fibers.[19] A typical step-profile circular waveguide is sketched in Fig. 8.

Snyder and Ruhl[1] have studied the case of a step-profile fiber whose axis lies along one of the principal axes of the dielectric tensor.[1] In such a waveguide $\epsilon_{yz} = 0$, and only the structural coupling terms contribute to the loss. In this section we consider the loss in fibers when $\epsilon_{yz} \neq 0$ and compare it with the loss in the cases in which $\epsilon_{yz} = 0$.

Even when $\epsilon_{yz} \neq 0$, the approximate Eqs. (14) have closed-form solutions. Coupling terms that are due both to ϵ_{yz} and to structural coupling contribute to the total loss. As a consequence of the orthogonality of the radiation modes involved in these two cases, the two contributions add without interference. The contribution to β^{im} from the $\epsilon_{yz} \neq 0$ coupling term, which couples the lowest-order y-polarized guided mode $e^{(0)}_{(y)y}$ with the x-polarized radiation mode having $\cos\phi$ symmetry, is

$$\beta^{\mathrm{im}}_{(y)2} = (\beta_{(y)0}\Delta_x^2\cot^2\alpha)\left[\frac{\pi W_y^2 J_0^2(U_y)}{V_y^2 J_1^2(U_y)}\right][|p_1|^2 J_1^2(U_x)]. \tag{33}$$

Equation (33) is obtained from Eq. (23) by the use of the expressions for LP modes $e^{(0)}_{(y)y}$ and $e^{(0)}_{(x)x}$ given in Eqs. (B24) and (B25) and the associated normalization integral and constant, $\langle e^{(0)2}_{(y)y}\rangle$ and N_q, given in Eqs. (B28) and (B29). The definition of the coefficient p_l is given by Eq. (B26). Note that, as in Eq. (24) for the planar waveguide, the expression for the loss contains a factor that is independent of modal parameters, one that is dependent only on the guided mode, and one that is dependent only on the radiation mode.

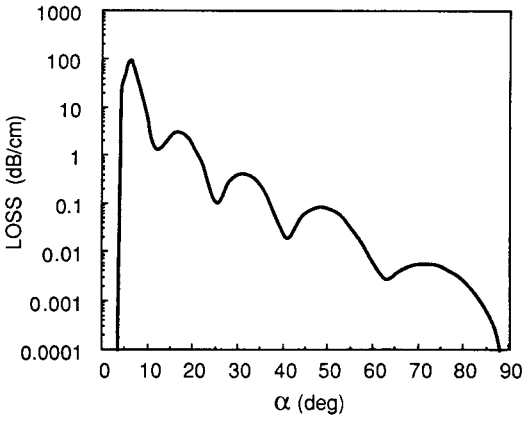

Fig. 7. Loss coefficient of the lowest-order leaky mode for the asymmetric waveguide in Fig. 6, where $\rho = 4.078$ μm, $\lambda = 0.6328$ μm, $n_{1,\mathrm{co}} = 2.281$, $n_{3,\mathrm{co}} = 2.174$. $\Delta_{x1} = \Delta_{y1} = 0.002$, and $\Delta_{x2} = \Delta_{y2} = 0.0005$.

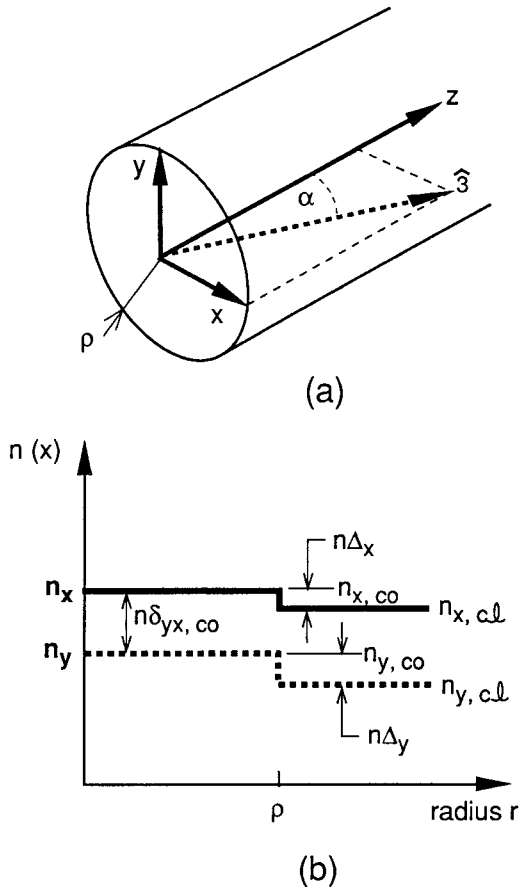

Fig. 8. (a) Birefringent fiber with radius ρ, (b) step-index profiles for the fiber.

When $\epsilon_{yz} = 0$, $e^{(0)}_{(y)y}$ couples only to the x-polarized radiation mode with $\sin(2\phi)$ symmetry, and the result for β^{im}, first given by Ruhl and Snyder,[9] is

$$\beta^{\text{im}}_{(y)2} = (\beta_{(y)0}\Delta_x{}^2\Delta_y)\left[\frac{\pi W_y{}^2 J_0{}^2(U_y)}{2V_y{}^4 J_1{}^2(U_y)}\right] \times \left\{|p_2|\left[\frac{\delta_{xz}}{\delta_{yx}}\frac{\Delta_y}{\Delta_x}U_x J_1(U_x) + \frac{\delta_{yz}}{\delta_{yx}}\frac{U_y J_1(U_y)}{J_0(U_y)}J_2(U_x)\right]\right\}^2, \tag{34a}$$

where in our case

$$\frac{\delta_{xz}}{\delta_{yx}} = -\cot^2\alpha, \tag{34b}$$

$$\frac{\delta_{yz}}{\delta_{yx}} = 1 - \cot^2\alpha. \tag{34c}$$

The total loss for $\epsilon_{yz} \neq 0$ is then the sum of the two contributions, Eqs. (33) and (34a).

As can be seen from Eqs. (33) and (34a), the major difference between the $\epsilon_{yz} \neq 0$ and $\epsilon_{yz} = 0$ cases arises from the first factor in each equation. The loss for $\epsilon_{yz} \neq 0$ is larger by Δ^{-1} unless α approaches $\pi/2$, as is borne out by Fig. 9, which compares the loss coefficient that is due to nonvanishing off-diagonal elements of the dielectric tensor with that resulting from structural coupling. The parameters of the waveguide are chosen to be the same as for one of the symmetric planar waveguides in Fig. 5 ($\Delta_x = \Delta_y = 0.002$), with the radius equal to the half-thickness of the symmetric planar waveguide.

Comparing Fig. 9 with the loss coefficient for the symmetric planar waveguide with $\Delta_x = \Delta_y = 0.002$ as shown in Fig. 5, we find that the loss in the fiber resembles closely the loss in the planar waveguide. However, α_{th} is smaller, which can be expected from the smaller b in the fiber for fixed V_y and from the expression for α_{th} given by Eq. (27), and the locations of the maxima and the zeros are shifted. It can also be shown that, for fixed waveguide parameters $\Delta, V(\Delta_x = \Delta_y = \Delta, V_x = V_y = V)$, the envelope of the loss in the fiber is smaller than that in the symmetric waveguide when $V < 1.1$, is larger when $V > 1.1$, and is approximated by $1.17g$ when $V \gg 1$, where g is the envelope function for the loss in a symmetric planar waveguide as given by Eq. (25).

As was the case for the planar waveguide, the loss coefficient for the anisotropic fiber becomes extremely large when $Q_z \to 0$ and the first antisymmetric mode is near cutoff. This behavior is a result of the factor $|p_l|^2$ in Eqs. (33) and (34a), where p_l, defined in Eq. (B26), is proportional to $1/J_{l-1}(V_x)$ and hence diverges when $V_x \to 2.405$, which is the cutoff condition for the first antisymmetric mode. This divergence in $|p_l|$ leads to a divergence in the loss coefficient unless $\epsilon_{yz} = 0$.

D. Symmetric Linear-Profile Waveguide

Thus far we have compared several types of waveguide, but all have had step profiles. In order to determine the effect of grading the refractive-index profile, we consider an analytically tractable case, the symmetric linear-index profile, illustrated in Fig. 10. This profile is defined by

$$f_i(x) = \begin{cases} |x|/\rho & |x| < \rho, \\ 1 & |x| > \rho \end{cases} \tag{35}$$

where $i = x, y$, and ρ is the half-thickness of the waveguide. The LP modes for this profile are presented in Appendix B. In order to have a closed-form expression for the loss, we assume here that $\Delta_1 = \Delta_3$, and hence $\Delta_x = \Delta_y$. For this profile, the overlap integral in Eq. (23), $\langle(\partial f_x/\partial x)e^{(0)}_{(y)y}e^{(0)}_{(x)x}\rangle$, reduces to $\int_0^1 e^{(0)}_{(x)x}e^{(0)}_{(y)y}dx$. Rather than carry out this complicated integration, we transform the coupling coefficient to a simpler form that involves inte-

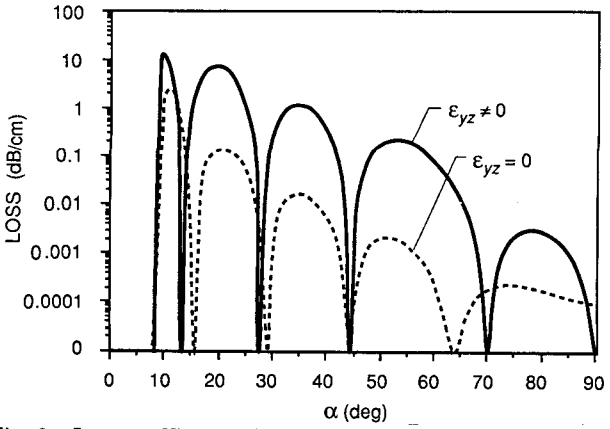

Fig. 9. Loss coefficient of the lowest-order leaky mode for the fiber shown in Fig. 8. The solid curve represents the loss that is due to nonvanishing off-diagonal dielectric tensor element ϵ_{yz}, while the dashed curve shows the structural loss that exists even when $\epsilon_{yz} = 0$. The waveguide parameters are chosen as $\rho = 2.039$ μm, $\lambda = 0.6328$ μm, $n_{1,\text{co}} = 2.281$, $n_{3,\text{co}} = 2.174$, $\Delta_1 = \Delta_3 = 0.002$.

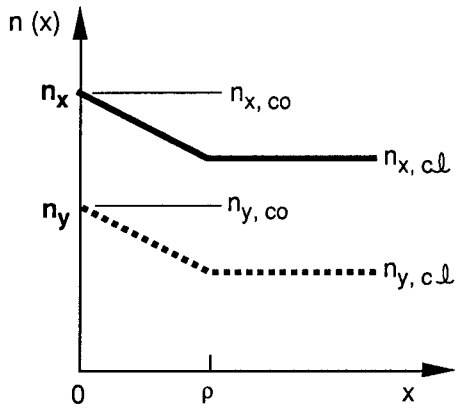

Fig. 10. Symmetric linear-index profile, where the half-thickness of the guiding layer is ρ.

gration only over the cladding region. Since $e^{(0)}_{(y)y}$ and $e^{(0)}_{(x)x}$ are degenerate, it can be derived from Eqs. (18) that

$$\langle(\epsilon_{xx} - \epsilon_{yy})e^{(0)}_{(x)x}e^{(0)}_{(y)y}\rangle = 0. \tag{36}$$

As we have assumed that $\Delta_1 = \Delta_3$, $(\epsilon_{xx} - \epsilon_{yy})$ is independent of x and can be taken out of the integral in Eq. (36), it follows that

$$\langle e^{(0)}_{(y)y}e^{(0)}_{(x)x}\rangle = 0. \tag{37}$$

Therefore the integral in the guiding layer is equal in magnitude and opposite in sign to the integral in the substrate, which is easier to evaluate because of the simpler form of the fields in the latter region. With this approach, and using the LP modes given in Eqs. (B30) and (B31), the expression for β^{im} given in Eq. (23) becomes

$$\beta^{\text{im}}_{(y)2} = (4\beta_{(y)0}\Delta_x{}^2\cot^2\alpha)\left[\frac{s_y{}^2(1)}{2\langle e^{(0)}_{(y)y}{}^2\rangle}\right] \times \left[\frac{Q_x}{(U_x{}^2 - U_y{}^2)^2}\right]\left\{\frac{[s_x'(1) + W_y s_x(1)]^2}{s_x'{}^2(1) + Q_x{}^2 s_x{}^2(1)}\right\}, \tag{38a}$$

where $s_i, i = x, y$ are combinations of the Airy functions defined by Eq. (B33), $\langle e^{(0)}_{(y)y}{}^2\rangle$ is given in Eqs. (B37), and s_i' is the derivative of the function s_i.

Similarly to those in Eq. (24) for the symmetric slab waveguide, the first three factors of Eq. (38a) behave like the envelope function g given by Eq. (25), and the last factor is comparable with the oscillatory function h given by Eq. (26). To compare the two envelope functions, we use the relation between $U_x{}^2$ and $U_y{}^2$ given in Table 1 and find that the ratio of the envelope function for linear profiles to the envelope function for step profiles is

$$\frac{g_{\text{lin}}}{g_{\text{step}}} \approx \frac{U_{x,\text{step}}{}^2}{(U_x{}^2 - U_y{}^2)^2_{\text{lin}}} = \frac{\Delta_y}{V_y{}^2\delta_{31,\text{co}}\sin^2\alpha}\left(1 + \frac{U_{y,\text{step}}{}^2\Delta_y}{V_y{}^2\delta_{31,\text{co}}\sin^2\alpha}\right), \tag{38b}$$

where we neglect the difference in the amplitudes of the bound-mode fields at $R = 1$, i.e., we take $s_y{}^2(1)/2\langle e^{(0)}_{(y)y}{}^2\rangle \approx (U_y{}^2/V_y{}^2)/(1 + 1/W_y)$. The difference comes from the overlap integral in Eq. (23), which is equal to the value of $e^{(0)}_{(y)y} \cdot e^{(0)}_{(x)x}$ at the interface in the cases of a step profile but is a weighted average of this product when the profile is graded. From Eq. (38b), we conclude that waveguides with linear profiles are less leaky than waveguides with step profiles when $V^2\delta_{31}/\Delta \gg 1$, such as for Ti:$LiNbO_3$ waveguides; but, if $V^2\delta_{31}/\Delta$ is of order unity, as is the case in a proton-exchanged waveguide, the sizes of the losses in waveguides with linear profiles and step profiles are comparable. The above statements are verified by Figs. 11 and 12, which show the plots of loss versus α for linear and step-profile waveguides with the same Δ and V, where $V(\delta_{31}/\Delta)^{1/2}$ is 14 in Fig. 11 and 0.95 in Fig. 12. Although the above conclusions are drawn for the case of linear profiles, we expect a similar trend for all graded profiles.

The linear graded profile again shows high loss when $Q_x \to 0$ and $s_x'(1) = 0$; the latter can be shown to be the cutoff condition for the first antisymmetric mode.

5. EXTENSIONS OF THE METHOD

A. Positive Uniaxial Waveguides

In the previous analysis in Subsection 4.D, we have assumed that the media are negative uniaxial. For a

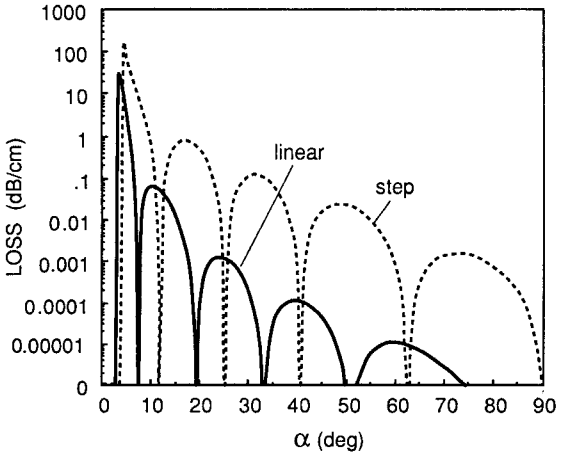

Fig. 11. Loss coefficient of the lowest-order leaky mode for the linear-profile waveguide shown in Fig. 10 (solid curve). The dashed curve shows the loss coefficient for a step-index waveguide with the same parameters, which are $\rho = 2.039$ μm, $\lambda = 0.6328$ μm, $n_{1,\text{co}} = 2.281$, $n_{3,\text{co}} = 2.174$, $\Delta_1 = \Delta_3 = 0.0005$. In this case $V\delta_{31}{}^{1/2}\Delta_1{}^{-1/2} = 14$, and hence the step-profile waveguide is much more leaky than the linear-profile waveguide, as shown in Eq. (38b).

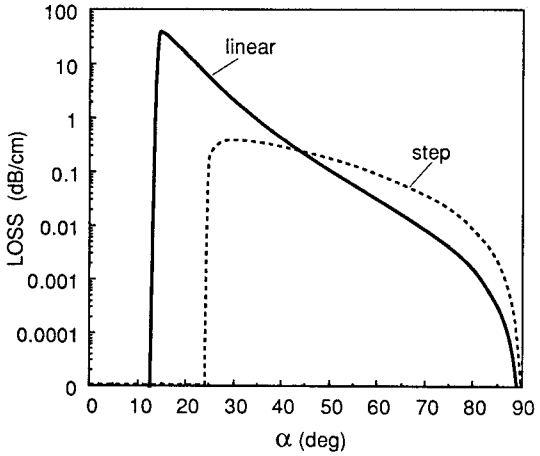

Fig. 12. Losses for a linear-profile (solid curve) and a step-profile (dashed curve) waveguide. The parameters for the two waveguides are the same as those of the two waveguides in Fig. 11, except that $\rho = 1$ μm and $n_{3,\text{co}} = 2.279$. $V\delta_{31}{}^{1/2}\Delta_1{}^{-1/2} = 0.95$ in this case, and thus the size of loss for the linear-profile is comparable with or larger than that for the step profile.

negative uniaxial waveguide as shown in Fig. 1, only the y-polarized modes are leaky, and the loss appears when α exceeds a threshold angle α_{th}. Analogously, for positive uniaxial waveguides, only the x-polarized modes are leaky, and the corresponding threshold angle for leakage is the same as the one in negative media given by Eq. (27). All the expressions for the leakage rate that are derived with negative uniaxial guides can also be used for positive uniaxial guides, provided that the coordinates x and y are interchanged. Thus, the loss in positive uniaxial waveguides behaves in the same way as in negative uniaxial waveguides with comparable anisotropy and index profiles.

B. Strongly Asymmetric Waveguides

The results in Sections 3 and 4 were derived under the assumptions of weak guidance and weak anisotropy. In many cases of practical interest one or both of these assumptions are violated to some degree. It is interesting to investigate the possibility of extending the analysis to those cases. In this section we discuss the case of a strongly asymmetric planar waveguide for which the weak-guidance assumption is violated at one interface, and then we touch on the question of strong birefringence.

A common type of waveguide is constructed by diffusing a dopant into a thin layer at the surface of a substrate, with air, or perhaps a low-index-of-refraction buffer, serving as the superstrate. Such a waveguide is shown schematically in Fig. 13. The thickness of the waveguide is ρ, and the profile heights at the interface between the guiding layer and the substrate, Δ_{x2} and Δ_{y2}, result from diffusion and are thus small; the sizes of Δ_{x1} and Δ_{y1}, the profile heights at $x = 0$ (the air–film interface), are of order unity. The material anisotropy, as in the previous cases, is assumed to be weak everywhere. In this case the only deviation from our previous model is the relaxation of the weak guidance assumption at one interface.

While $\Delta \ll 1$ is used in the previous analysis as a sufficient condition for the validity of the perturbation expansion (except for special points where the guided mode is degenerate with near-cutoff radiation modes), a necessary condition for valid approximation is only that the coupling terms on the RHS's of Eqs. (10) be small. For the planar waveguide shown in Fig. 13, the coupling terms given by Eqs. (11) reduce to

$$P_{xx}\bar{e}_x = \frac{\partial}{\partial x}\left[\left(1 - \frac{\epsilon_{xx}}{\epsilon_{zz}}\right)\frac{\partial \bar{e}_x}{\partial x}\right] - \frac{\partial}{\partial x}\left(\bar{e}_x \frac{\epsilon_{xx}}{\epsilon_{zz}}\frac{\partial}{\partial x}\ln \epsilon_{xx}\right), \quad (39a)$$

$$P_{xy}\bar{e}_y = i\beta \frac{\partial}{\partial x}\left(\frac{\epsilon_{yz}}{\epsilon_{zz}}\bar{e}_y\right), \quad (39b)$$

$$P_{yx}\bar{e}_x = \frac{k^2}{i\beta}\frac{\epsilon_{yz}}{\epsilon_{zz}}\frac{\partial}{\partial x}(\epsilon_{xx}\bar{e}_x), \quad (39c)$$

$$P_{yy}\bar{e}_y = 0. \quad (39d)$$

Examining Eqs. (39), we find that all coupling terms are small except the second term on the RHS of Eq. (39a), the expression for $P_{xx}\bar{e}_x$. Therefore this term should be added to the RHS of Eq. (14a) for the zeroth-order x-polarized mode. The zeroth-order modes of a step profile obtained in this way are the ordinary TM modes of an isotropic waveguide, given in Eqs. (B17) and (B20).

After moving the second $P_{xx}\bar{e}_x$ term to the zeroth-order equations, we can repeat the derivation leading from Eqs. (18) to Eq. (23) and find the second-order correction to $\beta_{(y)}$ to be

$$\beta^{\text{im}}_{(y)2} = \beta_{(y)0}\frac{\pi\rho^2\Delta_{x2}\cot^2\alpha}{\langle e^{(0)2}_{(y)y}\rangle}\frac{\left\langle \frac{\epsilon_{xx,\text{co}}}{\epsilon_{xx}}\frac{\partial f_x}{\partial x}e^{(0)}_{(y)y}e^{(0)}_{(x)x}\right\rangle^2}{N_{q2}Q_{x2}}, \quad (40a)$$

where N_{q2} is defined by

$$\langle e^{(0)}_{(x)x}{}^*(Q_{x2}')e^{(0)}_{(x)x}(Q_{x2})\rangle = N_{q2}\delta(Q_{x2} - Q_{x2}'). \quad (40b)$$

Note that, with this definition, $f(x)$ is no longer of order unity, having a maximum value Δ_{x1}/Δ_{x2}. In deriving Eq. (40a) we have not assumed any particular form for the index profile, and hence it can be applied to graded as well as to step profiles. Comparing Eq. (40a) with Eq. (23), the loss for $\Delta \ll 1$, we find that the only difference is that the overlap integral is modified by $\epsilon_{xx,\text{co}}/\epsilon_{xx}$ in Eq. (40a).

We need to check the criteria for the validity of the perturbation eigenvalues, i.e., $|\beta_{(y)1}|, |\beta_{(y)2}| \ll \beta_{(y)0}$. It can be shown that the first-order correction to $\beta_{(y)}$, $\beta_{(y)1}$ is proportional to $\langle e^{(0)}_{(i)i}P_{ii}e^{(0)}_{(i)i}\rangle$ and therefore vanishes in this case because $P_{yy}e^{(0)}_{(y)y} = 0$. The real and imaginary parts of $\beta_{(y)2}$ are of the same order, and thus we check only the imaginary part. From Eq. (40a) we see that, in order to prove that $|\beta^{\text{im}}_{(y)2}| \ll \beta_{(y)0}$, we need to demonstrate that the product $\Delta_x(\partial f_x/\partial x)e^{(0)}_{(y)y}e^{(0)}_{(x)x}$ in the overlap integral is much smaller than unity. On the small Δ side the product is small, while on the other side, where Δ is of order unity, if it can be shown that the transverse fields are small in regions where the index of refraction is changing, then the product is small. We now specialize to the case of step-profile waveguides. For planar waveguides with step-index profiles, the index of refraction varies only at the interfaces between the guiding layer and the substrates or superstrates. In addition, because the guide is strongly asymmetric, $U_y \ll V_{y1}$, $U_x \ll V_{x1}$, and hence W_{y1} and W_{x1} can be approximated by V_{y1} and V_{x1}. In these limits it can be shown from Eqs. (B6) and (B20) that, at fixed V_x and V_y, the magnitude of the transverse fields, $e^{(0)}_{(i)i}$ at $x = 0$ (where Δ is of order unity), is proportional to $(\Delta_{i2}/\Delta_{i1})^{1/2}$ (notice that $e^{(0)}_{(i)i}$ has been set to be of order unity at the small Δ

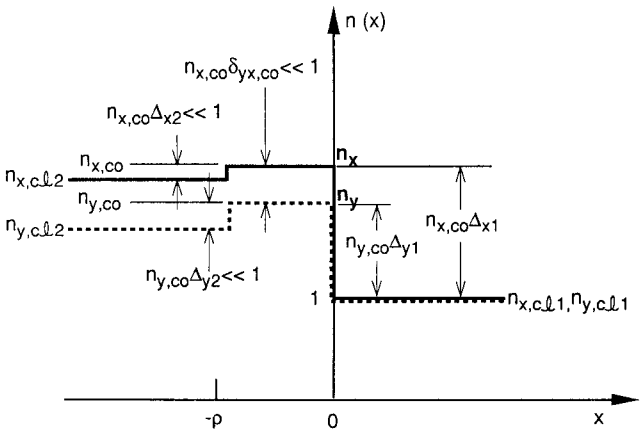

Fig. 13. Index profile for a strongly asymmetric planar waveguide, where the superstrate is air. $\Delta_{x2}, \Delta_{y2} \ll 1$, but Δ_{x1} and Δ_{y1} are of the order unity.

interface), so that $\Delta_x(\partial f_x/\partial x)e^{(0)}_{(y)y}e^{(0)}_{(x)x}$ is approximately proportional to $(\Delta_{x2}\Delta_{y2})^{1/2}$ and is small there.

So far we have proved that the perturbation analysis can be applied in the case of strongly asymmetric step-index waveguides, with one extra term retained in the zeroth-order equations for the x-polarized LP modes. To calculate the loss we use Eqs. (B6) and (B20) for $e^{(0)}_{(y)y}$ and $e^{(0)}_{(x)x}$ and use the normalization constants given by Eqs. (B17) and (B27) in Eq. (40a), which becomes

$$\beta^{\mathrm{im}}_{(y)2} = (4\beta_{(y)0}{\Delta_{x2}}^2 \cot^2\alpha)\left[\frac{U_y{}^2W_{y2}}{V_{y2}{}^2(1+W_{y2})}\right]\eta^2 \times \frac{(1-\eta^{-1}\sin U_x)^2}{Q_x[1+(V_{x2}{}^2/Q_x{}^2)\cos^2 U_x]}, \tag{41a}$$

where

$$\eta = \frac{1}{2}\left(\frac{\epsilon_{xx,\mathrm{co}}}{\epsilon_{xx,\mathrm{cll}}} + \frac{\epsilon_{xx,\mathrm{cll}}}{\epsilon_{xx,\mathrm{co}}}\right)\frac{V_{y2}U_x}{V_{x2}{}^2}. \tag{41b}$$

As was the case for the weakly guiding waveguide to first order in Δ_{i2} and δ_{31}, the results of the perturbation analysis agree with the exact results from Appendix C.

Now we compare Eq. (41a) with its counterpart for symmetric planar waveguides, Eq. (24). Equation (41a) looks similar to the loss for a symmetric waveguide with profile heights equal to Δ_{x2} and Δ_{y2} and half-thickness equal to ρ, except for the last oscillatory factor and the factor η^2 in the envelope. η is of order unity at $\sigma = 0$ and increases monotonically with α. When $\delta_{31} \gg \Delta_{i2}, \Delta_{y2}, \eta \approx (\Delta_{y2}\delta_{31})^{1/2}\sin\alpha/\Delta_{i2} \gg 1$, so that the loss coefficient of the strongly asymmetric waveguide can be considerably larger than that of a weakly asymmetric waveguide.

The envelope becomes flat in strongly asymmetric guides because η increases with α and hence lifts the envelope. η is independent of Δ_{x1} and Δ_{y1} in the limit $\Delta_{x1}, \Delta_{y1} \gg \Delta_{x2}, \Delta_{y2}$, since, from the definition of U_x given in Table 2 and the definitions of V_{y2} and Δ_y in Table 1, it can be shown that U_x does not depend on Δ_{x1} and Δ_{y1} in that limit and V_{y2}/V_{x2} is always independent of Δ_{x1} and Δ_{y1}. The other factors in the envelope of the loss given by Eq. (41a) are also independent of Δ_{x1} and Δ_{y1}; thus the envelope of the loss does not depend on the large profile heights. η^2 is also the ratio of the envelope of the loss given in Eq. (41a) to g, the envelope function for symmetric waveguides given by Eq. (25). It has been mentioned before that this ratio is proportional to $\delta_{31}\sin^2\alpha/\Delta_{i2}$, which is of order unity when the anisotropy is comparable with the small profile heights, but it is much larger than unity when $\delta_{31} \gg \Delta_{i2}$, unless α is small.

There are two terms in the numerator of the last oscillatory factor in Eq. (41a); the first one is a constant and arises from the integral over the region near $x = 0$, where Δ is of order unity, and the second one is an oscillatory function of α with a magnitude η^{-1} and comes from the integral over the region near the small Δ interface. At small α the two terms are comparable in magnitude. As α increases, the first term becomes increasingly important and the oscillation becomes weaker, until, if $\delta_{31} \gg \Delta_{i2}$, the oscillation disappears. Figure 14 shows the loss coefficient of a strongly asymmetric waveguide, with air as the superstrate. We see that the oscillations decrease as α increases, and the envelope is quite flat as a function of α, compared with the loss for symmetric waveguides given in Fig. 4.

We can reach the following conclusions: For a strongly asymmetric waveguide, the loss is insensitive to the large profile height. When the anisotropy δ is of the same order as the small profile height Δ, the size of the loss for a strongly asymmetric waveguide is comparable with that of a symmetric waveguide with a profile height equal to Δ. When $\delta \gg \Delta$, the leakage rate for the strongly asymmetric waveguide is larger than that of the symmetric waveguide by a factor of $\delta\sin^2\alpha/\Delta$. In the latter case burying the waveguide with a buffer layer between the air and the guiding layer will reduce the loss substantially.

For a general waveguide with one large index step, we would expect the behavior of the coupling to be similar to that of a step-index waveguide. The results of perturbation calculations should be accurate for asymmetric planar waveguides if Δ is small at least on one side, if Eq. (23) for the coupling coefficient is replaced with the modified form, Eq. (40).

Waveguides with highly birefringent cores could also occur in practice. In the case of strong anisotropy but weak guidance, the perturbation method is still useful. The modal fields and the propagation constant can be evaluated by methods similar to those that lead to Eq. (40), incorporating modified forms of the $P_{ij}\bar{e}_j$ terms. These results will be discussed in a future publication.

5. SUMMARY

Guided modes of anisotropic waveguides are often leaky because of coupling to degenerate orthogonally polarized radiation modes. We have extended the calculation of these losses that was first presented in Ref. 1 to include waveguides with arbitrarily oriented dielectric tensors. When a principal axis is not aligned with the waveguide axis, the loss arising from the off-axis components of the dielectric tensor is much larger than the structural loss present in two-dimensional anisotropic waveguides that have a principal axis aligned with the waveguide axis. We have derived a simplified expression for the loss, which shows that the coupling occurs in regions where the refractive index is spatially varying. Application of these results to step-index planar waveguides, for which exact

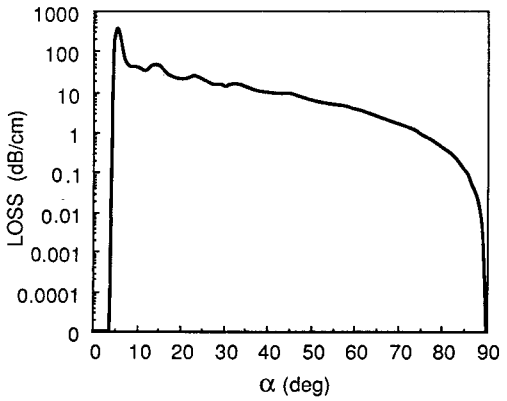

Fig. 14. Loss coefficient of the lowest-order leaky mode of the strongly asymmetric waveguide shown in Fig. 13, where $\rho = 6\ \mu$m, $\lambda = 0.6328\ \mu$m, $n_{1,\mathrm{co}} = 2.281$, $n_{3,\mathrm{co}} = 2.174$, $n_{1,\mathrm{cl2}} = 2.2799$, $n_{3,\mathrm{cl2}} = 2.1697$, and $n_{1,\mathrm{cll}} = n_{3,\mathrm{cll}} = 1$.

solutions are available, shows that the approximate results are accurate in the limit of small anisotropy even for strongly asymmetric waveguides, as long as one of the interfaces is weakly guiding.

Examples drawn from planar and fiber waveguides illustrate general trends for the dependence of the loss on the profile height Δ, the angle between the optical axis and the waveguide axis α, and the anisotropy δ. For symmetric planar waveguides, the loss is proportional to $\Delta^2 \cot^2 \alpha$. For strongly asymmetric waveguides, the loss is insensitive to the large-profile height and proportional to the square of the small-profile height Δ. Compared with a symmetric waveguide that has the same Δ, the loss of a strongly asymmetric waveguide is much larger when $\Delta \ll \delta$ but is of the same order when $\Delta \approx \delta$. The loss for a birefringent fiber with $\alpha \neq 0$ is of the order Δ^{-1} larger than that of a fiber with $\alpha = 0$ and is comparable with that of a symmetric planar waveguide that has similar profile height and anisotropy. The loss of a planar waveguide with a linearly graded refractive-index profile is much smaller than that of a step profile when $2\pi\rho\delta^{1/2}/\lambda \gg 1$ but is comparable when this quantity is of order unity.

APPENDIX A: INTEGRAL EXPRESSIONS FOR THE COUPLED FIELDS AND THE PROPAGATION CONSTANT

Snyder and Ruhl[1] approximate the j component of a predominantly i-polarized leaky mode (i and j are set to be y and x, respectively) by the integral

$$e_{(i)j}^{(1)} = \int_0^{\rho k n_{jd}} a_q e_{(j)j}^{(0)}(Q_j) \mathrm{d}Q_j , \tag{A1}$$

where $e_{(j)j}^{(0)}(Q_j)$ are the continuum solutions to the homogeneous Eq. (14a). To find the modal coefficients a_q, one first substitutes the form given in Eq. (A1) for $e_{(i)j}^{(1)}$ in Eq. (14b), then multiplies Eq. (14b) by $e_{(j)j}^{(0)*}(Q_j')$. With the orthogonality relation

$$\langle e_{(j)j}^{(0)*}(Q_j') e_{(j)j}^{(0)}(Q_j) \rangle = N_q \delta(Q_j - Q_j') , \tag{A2}$$

a_q is obtained as

$$a_q = \frac{\langle e_{(j)j}^{(0)*}(Q_j) P_{ji} e_{(i)i}^{(0)} \rangle}{N_q(\beta_{(j)0,q}{}^2 - \beta_{(i)0}{}^2)} , \tag{A3}$$

and the j component of the leaky mode becomes

$$e_{(i)j}^{(1)} = -\int_0^{k n_{j,\mathrm{cl}}} \frac{\rho^2 \langle e_{(j)j}^{(0)*}(Q_j) P_{ji} e_{(i)i}^{(0)} \rangle e_{(j)j}^{(0)}(Q_j)}{2 Q_j N_q (\beta_{(j)0,q} - \beta_{(i)0})} \mathrm{d}\beta_{(j)0,q} , \tag{A4}$$

where the relation $dQ_j = -\rho^2 \beta_{(j)0,q} \mathrm{d}\beta_{(j)0,q}/Q_j$ has been used. In the expression for $\beta_{(i)2}$ given by Eq. (15), only the third term can result in an imaginary component. Thus, by taking $e_{(i)j}^{(1)}$ in the form given in (A4), one is led to

$$\beta_{(i)2}^{\mathrm{im}} = \frac{1}{2\beta_{(i)0} \langle e_{(i)i}^{(0)\,2} \rangle} \mathrm{Im}\left[\int_0^{k n_{j,\mathrm{cl}}} \frac{\rho^2 |\langle e_{(j)j}^{(0)*}(Q_j) P_{ji} e_{(i)i}^{(0)} \rangle|^2}{2 Q_j N_q (\beta_{(j)0,q} - \beta_{(i)0})} \mathrm{d}\beta_{(j)0,q} \right] , \tag{A5}$$

where the relation

$$\langle e_{(j)j}^{(0)*}(Q_j) P_{ji} e_{(i)i}^{(0)} \rangle = \langle e_{(i)i}^{(0)*} P_{ij} e_{(j)j}^{(0)}(Q_j) \rangle^* \tag{A6}$$

is used. Equation (A6) results from the requirement that the perturbative modes be orthogonal to each other and is correct to lowest order in Δ and δ. Therefore the function to be integrated in Eq. (A5) is real. If $\beta_{(i)0} > k n_{j,\mathrm{cl}}$, the integral in Eq. (A5) is real since the contour is on the real axis only, while for $\beta_{(i)0} < k n_{j,\mathrm{cl}}$, deformation of the contour around the pole $\beta_{(j)0,q} = \beta_{(i)0}$ gives rise to an imaginary part of the integral. Thus we can define a threshold value for $\beta_{(i)0}$, β_{th}, as

$$\beta_{\mathrm{th}} = k(\epsilon_{jj,\mathrm{cl}})^{1/2} = k n_{j,\mathrm{cl}} , \tag{A7}$$

such that for $\beta_{(i)0} > \beta_{\mathrm{th}}$ the imaginary part of the propagation constant vanishes, while for $\beta_{(i)0} < \beta_{\mathrm{th}}$ the imaginary part of the propagation constant is given by

$$\beta_{(i)2}^{\mathrm{im}} = \frac{\pi\rho^2}{2\beta_{(i)0}} \frac{|\langle e_{(j)j}^{(0)*}(Q_j) P_{ji} e_{(i)i}^{(0)} \rangle|^2}{2 N_q Q_j \langle e_{(i)i}^{(0)\,2} \rangle} , \qquad \beta_{(j)0,q} = \beta_{(i)0} . \tag{A8}$$

The correction to the modal field that comes from the coupling between $e_{(i)i}^{(0)}$ and the i-polarized radiation modes can be obtained in the same way, and the result is same as Eq. (A4) with j replaced by i. However, this $e_{(i)i}^{(1)}$ will not introduce the loss to the mode. To see this, we can go through a similar process from Eqs. (A5)–(A8) and find that there is no pole in the contour of the integral in Eq. (A5) if j is replaced by i, because no i-polarized radiation mode can be degenerate with $e_{(i)i}^{(0)}$.

APPENDIX B: LP MODES

The LP modes $e_{(y)y}^{(0)}$ and $e_{(x)x}^{(0)}$ are the solutions of Eq. (14a). In this appendix we present the expressions for LP modes of several model-guiding structures. In these expressions a normalized transverse coordinate, $\bar{x}$, is defined by $\bar{x} = x/\rho$ for planar waveguides, and R is defined by $R = r/\rho$ for waveguides of circular cross section, where ρ is a characteristic dimension of the guiding region that is defined below.

1. Symmetric Step-Profile Planar Waveguide

A symmetric step-profile planar waveguide is shown in Fig. 2. An even-guided LP mode of the y polarization has the form[15]

$$e_{(y)y}^{(0)} = \begin{cases} \cos(U_y \bar{x}) & |\bar{x}| < 1 \\ \cos(U_y) \exp[-W_y(|\bar{x}| - 1)] & |\bar{x}| > 1 \end{cases} , \tag{B1}$$

and an odd x-polarized radiation mode is given by

$$e_{(x)x}^{(0)} = \begin{cases} \sin(U_x \bar{x}) & |\bar{x}| < 1 \\ \dfrac{\bar{x}}{|\bar{x}|} \sin(U_x) \dfrac{\sin[Q_x(|\bar{x}| - 1) + \phi_x]}{\sin(\phi_x)} & |\bar{x}| > 1 \end{cases} , \tag{B2}$$

where ϕ_x satisfies the relation $\cot(\phi_x) = U_x \cot(U_x)/Q_x$ and the eigenvalue equation for the guided mode is

$$\tan(U_y) = \frac{W_y}{U_y} . \tag{B3}$$

The normalization integral and constant are

$$\langle e_{(y)y}^{(0)\,2} \rangle = \frac{\rho}{2}\left(1 + \frac{1}{W_y}\right) , \tag{B4}$$

$$N_q = \frac{\pi\rho}{2}\left[1 + \frac{V_x^2}{Q_x{}^2} \cos^2(U_x)\right] , \tag{B5}$$

where ρ is the half-thickness of the symmetric waveguide.

2. Asymmetric Step-Profile Planar Waveguide

For an asymmetric planar waveguide as illustrated in Fig. 6, the guided LP mode $e^{(0)}_{(y)y}$ is given by[16]

$$e^{(0)}_{(y)y} = \begin{cases} \dfrac{V_{y2}}{V_{y1}} \exp(-W_{y1}\bar{x}) & \bar{x} > 0 \\ \dfrac{V_{y2}}{U_y} \cos(U_y\bar{x} + \phi_a) & 0 > \bar{x} > -1, \\ \exp[W_{y2}(\bar{x} + 1)] & \bar{x} < -1 \end{cases} \tag{B6}$$

where $\phi_a = \cos^{-1}(U_y/V_{y1})$, and the normalization integral is given by

$$\langle e^{(0)\,2}_{(y)y} \rangle = \frac{\rho}{2} \frac{V_{y2}^2}{U_y^2} \left(1 + \frac{1}{W_{y1}} + \frac{1}{W_{y2}} \right), \tag{B7}$$

where ρ is the thickness of the asymmetric waveguide. The eigenvalue equation for this mode is given by

$$\cos(U_y) = \frac{U_y^2 - W_{y1}W_{y2}}{V_{y1}V_{y2}}. \tag{B8}$$

There are two kinds of radiation mode. The first kind decays in one of the cladding regions (in the following examples we choose $\bar{x} > 0$ as the side where the modes decay) and oscillates in the other. These modes exist for $kn_{x,\mathrm{cl1}} < \beta_{(x)0} < kn_{x,\mathrm{cl2}}$ (we have assumed that $n_{x,\mathrm{cl1}} < n_{x,\mathrm{cl2}}$) and have the forms

$$e^{(0)}_{(x)x} = \begin{cases} \exp(-W_{x1}\bar{x}) & \bar{x} > 0 \\ \dfrac{\sin(U_x\bar{x} + \phi_{x1})}{\sin(\phi_{x1})} & 0 > \bar{x} > -1, \\ -\dfrac{\sin(U_x - \phi_{x1})}{\sin(\phi_{x1})} \dfrac{\sin[Q_x(\bar{x} + 1) + \phi_{x2}]}{\sin(\phi_{x2})} & \bar{x} < -1 \end{cases} \tag{B9}$$

where

$$\cot(\phi_{x1}) = -\frac{W_{x1}}{U_x}, \tag{B10}$$

$$\cot(\phi_{x2}) = -\frac{U_x}{Q_{x2}} \cot(U_x - \phi_{x1}). \tag{B11}$$

The normalization constant of the above mode is

$$N_{q2} = \frac{\pi\rho}{2} \frac{V_{x1}^2}{U_x^2} \left[1 + \frac{V_{x2}^2}{Q_{x2}^2} \cos^2(U_x - \phi_{x1}) \right]. \tag{B2}$$

The other kinds of radiation mode, oscillatory in both superstrates and substrates, exist when $\beta_{(x)0} < kn_{x,\mathrm{cl1}}$ and have the forms[16]

$$e^{(0)}_{(x)x} = \begin{cases} \cos(Q_{x1}\bar{x}) + \dfrac{U_x}{Q_{x1}} F_m \sin(Q_{x1}\bar{x}) & \bar{x} > 0 \\ \cos(U_x\bar{x}) + F_m \sin(U_x\bar{x}) & 0 > \bar{x} > -1, \\ [\cos(U_x) - F_m \sin(U_x)] \dfrac{\cos[Q_{x2}(\bar{x} + 1) + \phi_x']}{\cos(\phi_x')} & \bar{x} < -1 \end{cases} \tag{B13}$$

where

$$\tan(\phi_x') = -\frac{U_x}{Q_{x2}} \tan(U_x + \phi_{fm}) \tag{B14}$$

and $\phi_{fm} = \cos^{-1}[1/(1 + F_m^2)^{1/2}]$. There are two types of mode, with F_m, $m = 1, 2$ representing two orthogonal solutions chosen in such a way that in the limit of a symmetric waveguide even and odd radiation modes result. The above requirement yields the following expressions for F_1 and F_2:

$$F_{1,2} = \frac{V_{x2}^2 \cos(2U_x) + (Q_{x2}/Q_{x1})V_{x1}^2 \pm [V_{x2}^4 + 2(Q_{x2}/Q_{x1})V_{x1}^2V_{x2}^2 \cos(2U_x) + (Q_{x2}^2/Q_{x1}^2)V_{x1}^4]^{1/2}}{V_{x2}^2 \sin(2U_x)}, \tag{B15}$$

where for F_1 the positive sign is used and for F_2 the negative sign is used. The corresponding normalization constants are

$$N_{q2} = \frac{\pi\rho}{2}(1 + F_m^2) \left[1 + \frac{V_{x2}^2}{Q_{x2}^2} \sin^2(U_x + \phi_{fm}) + \frac{Q_{x1}}{Q_{x2}} \left(1 + \frac{V_{x1}^2}{Q_{x1}^2} \frac{F_m^2}{1 + F_m^2} \right) \right]. \tag{B16}$$

3. Strongly Asymmetric Step-Profile Planar Waveguide

In strongly asymmetric waveguides the profile height Δ is small on one side only, as is shown in Fig. 13. The guided LP modes of the TE polarization can be deduced directly from those for weakly guiding waveguides by taking the limit $\Delta_{x2}, \Delta_{y2} \ll \Delta_{x1}, \Delta_{y1}$. The expression for the modal field, Eq. (B6), remains unchanged, while the normalization integral, Eq. (B), becomes

$$\langle e^{(0)\,2}_{(y)y} \rangle = \frac{\rho}{2} \frac{V_{y2}^2}{U_y^2} \left(1 + \frac{1}{W_{y2}} \right), \tag{B17}$$

and the eigenvalue equation, Eq. (B8), becomes

$$\cos(U_y) = -\frac{W_{y2}}{V_{y2}}. \tag{B18}$$

The LP radiation modes of the TM polarization, $e^{(0)}_{(x)x}$, are not solutions of Eq. (18b) anymore; instead they satisfy

$$(\nabla_t^2 + k^2\epsilon_{xx} - \beta_{(x)0}^2) e^{(0)}_{(x)x} = -\frac{\partial}{\partial x} \left(e^{(0)}_{(x)x} \frac{\partial \ln \epsilon_{xx}}{\partial x} \right), \tag{B19}$$

as is discussed in Section 5. Using $U_x, W_{x2}, V_{x2} \ll V_{x1}$, and

$V_{x1} \approx W_{x1}$, we derive from Eq. (B19)

$$e^{(0)}_{(x)x} = \begin{cases} \dfrac{\epsilon_{xx,\mathrm{co}}}{\epsilon_{xx,\mathrm{cl1}}} \dfrac{U_x}{V_{x1}} \exp(-W_{x1}\bar{x}) & \bar{x} > 0 \\ \dfrac{U_x}{V_{x1}} \dfrac{\cos(U_x\bar{x} + \phi_{x3})}{\cos(\phi_{x3})} & 0 > \bar{x} > -1, \\ \dfrac{\epsilon_{xx,\mathrm{co}}}{\epsilon_{xx,\mathrm{cl1}}} \sin(U_x) \dfrac{\cos[Q_{x2}(\bar{x}+1) + \phi_{x4}]}{\cos(\phi_{x4})} & \bar{x} < -1 \end{cases} \tag{B20}$$

$$N_{q2} = \frac{\pi\rho}{2} \frac{\epsilon_{xx,\mathrm{co}}{}^2}{\epsilon_{xx,\mathrm{cl1}}{}^2} \left[1 + \frac{V_{x2}{}^2}{Q_{x2}{}^2} \cos^2(U_x) \right], \tag{B21}$$

where ϕ_{x3} and ϕ_{x4} are determined from the continuity of the derivative of $e^{(0)}_{(x)x}$ at the two interfaces, obeying

$$\tan(\phi_{x3}) = \frac{\epsilon_{xx,\mathrm{co}}}{\epsilon_{xx,\mathrm{cl1}}} \frac{W_{x1}}{U_x}, \tag{B22}$$

$$\tan(\phi_{x4}) = -\frac{U_x}{Q_{x2}} \tan(U_x - \phi_{x3}). \tag{B23}$$

Notice that $e^{(0)}_{(x)x}$ is not continuous at the large Δ interface, but $\epsilon_{xx} e^{(0)}_{(x)x}$ is.

4. Step-Profile Circular Fiber

For the circular fiber depicted in Fig. 8, the y-polarized guided LP mode has the form[1]

$$e^{(0)}_{(y)y} = \begin{cases} \dfrac{J_{l_y}(U_y R)}{J_{l_y}(U_y)} G_{l_y}(\phi) & R < 1 \\ \dfrac{K_{l_y}(U_y R)}{K_{l_y}(W_y)} G_{l_y}(\phi) & R > 1 \end{cases}, \tag{B24}$$

and the x-polarized radiation mode is given by

$$e^{(0)}_{(x)x} = \begin{cases} p_{l_x} J_{l_x}(U_x R) G_{l_x}(\phi) & R < 1 \\ [J_{l_x}(Q_x R) + q_{l_x} H^{(1)}_{l_x}(Q_x R)] G_{l_x}(\phi) & R > 1 \end{cases}, \tag{B25}$$

where the constants p_l and q_l are

$$p_{l_x} = \frac{2i}{\pi} [U_x J_{l_x+1}(U_x) H^{(1)}_{l_x}(Q_x) - Q_x J_{l_x}(U_x) H^{(1)}_{l_x+1}(Q_x)]^{-1}, \tag{B26}$$

$$q_{l_x} = \frac{i\pi}{2} p_{l_x} [U_x J_{l_x+1}(U_x) J_{l_x}(Q_x) - Q_x J_{l_x}(U_x) J_{l_x+1}(Q_x)], \tag{B27}$$

and $G_l(\phi) = \cos(l\phi)$ for even modes, $G_l(\phi) = \sin(l\phi)$ for odd modes. The normalization constants are

$$\langle e^{(0)}_{(y)y}{}^2 \rangle = \pi\rho^2 \frac{V_y{}^2}{W_y{}^2} \frac{J_1{}^2(U_y)}{J_0{}^2(U_y)}, \tag{B28}$$

$$N_q = t \frac{\pi\rho^2}{Q_x}, \tag{B29}$$

where $t = 1, 2$ for $l \geq 1$ and $l = 0$, respectively, and ρ is the radius of the circular waveguide.

5. Symmetric Linear-Profile Planar Waveguide

A symmetric linear-index profile is shown in Fig. 10. An even-guided mode of the y polarization for waveguides with such a profile has the field expression[20]

$$e^{(0)}_{(y)y} = \begin{cases} s_y(|\bar{x}|) & |\bar{x}| < 1 \\ s_y(1)\exp[-W_y(|\bar{x}| - 1)] & |\bar{x}| > 1 \end{cases}, \tag{B30}$$

and the modal solution for an odd x-polarized radiation mode is

$$e^{(0)}_{(x)x} = \begin{cases} \bar{x}/|\bar{x}| s_x(|\bar{x}|) & |\bar{x}| < 1 \\ \bar{x}/|\bar{x}| s_x(1) \dfrac{\sin[Q_x(|\bar{x}| - 1) + \phi_x]}{\sin(\phi_x)} & |\bar{x}| > 1 \end{cases}, \tag{B31}$$

where

$$\cot(\phi_x) = \frac{s_x'(1)}{Q_x S_x(1)}, \tag{B32}$$

$$s_j(\bar{x}) = Ai\left[\left(\bar{x} - \frac{U_j^2}{V_j^2}\right) V_j^{2/3}\right] + d_j Bi\left[\left(\bar{x} - \frac{U_j^2}{V_j^2}\right) V_j^{2/3}\right], \quad j = x, y, \tag{B33}$$

and $Ai(x)$ and $Bi(x)$ are Airy functions. The eigenvalue equation for $e^{(0)}_{(y)y}$ is given by

$$Ai'\left(\frac{V_y^2}{V_y^{4/3}}\right) + d_y Bi'\left(\frac{W_y^2}{V_y^{4/3}}\right) = \frac{W_y}{V_y^{2/3}} \left[Ai\left(\frac{W_y^2}{V_y^{4/3}}\right) + d_y Bi\left(\frac{W_y^2}{V_y^{4/3}}\right) \right]. \tag{B34}$$

The coefficients d_j are given by

$$d_y = -\frac{Ai'(-U_y{}^2/V_y{}^{4/3})}{Bi'(-U_y{}^2/V_y{}^{4/3})}, \tag{B35}$$

$$d_x = -\frac{Ai(-U_x{}^2/V_x{}^{4/3})}{Bi(-U_x{}^2/V_x{}^{4/3})}. \tag{B36}$$

The normalization integral $\langle e^{(0)}_{(y)y}{}^2 \rangle$ is

$$\langle e^{(0)}_{(y)y}{}^2 \rangle = \rho \left(\frac{W_y{}^2}{V_y{}^2} s_y(1) + \frac{U_y{}^2}{V_y{}^2} s_y(0) - \frac{1}{V_y{}^2} s_y'(1) \right) + \frac{\rho}{2W_y} s_y{}^2(1), \tag{B37}$$

and the normalization constant of the radiation mode $e^{(0)}_{(x)x}$ is

$$N_q = \frac{\pi\rho}{2} \left(s_x{}^2(1) + \frac{s_x'{}^2(1)}{Q_x{}^2} \right). \tag{B38}$$

APPENDIX C: EXACT SOLUTION FOR THE PROPAGATION CONSTANT OF AN ASYMMETRIC PLANAR WAVEGUIDE

Marcuse[2] has given the exact solution for the propagation constants and the modal fields of symmetric waveguides. Following his procedure, we can derive the exact solution for asymmetric waveguides. Here we list only the result for the propagation constant, which satisfies the following equation:

$$AD - CB = 0, \tag{C1}$$

where

$$A = -\frac{h_1 \cot^2 \alpha}{F_1 \epsilon_{xx,\mathrm{co}}}\left(\cos U_o - \frac{G}{F_2}\frac{W_{o2}}{U_o}\sin U_o\right) + \frac{h_2 \cot^2 \alpha}{F_2 \epsilon_{\mathrm{xx,co}}}\left(\cos U_e - \frac{\epsilon_{xx,\mathrm{cl1}}}{\epsilon_{xx,\mathrm{co}}}\frac{G}{F_1}\frac{W_{e1}}{U_e}\sin U_e\right); \quad \text{(C2)}$$

$$B = -\left(\frac{W_{o1}}{F_1} + \frac{W_{o2}}{F_2}\right)\frac{G}{U_o}\cos U_o + \left(\frac{G^2}{F_1 F_2}\frac{W_{o1}W_{o2}}{U_o^2} - 1\right)\sin U_o - \frac{\rho^2 k^2 h_1 h_2 \cot^2 \alpha}{\epsilon_{xx,\mathrm{co}} F_1 F_2 U_o}\frac{\sin U_e}{U_e}; \quad \text{(C3)}$$

$$C = \frac{\rho^2 k^2 h_1 h_2 \cot^2 \alpha}{\epsilon_{xx,\mathrm{co}} F_1 F_2}\frac{\sin U_o}{U_o} + \left(\frac{\epsilon_{xx,\mathrm{cl1}}}{\epsilon_{xx,\mathrm{co}}}\frac{G}{F_1}W_{e1} + \frac{\epsilon_{\mathrm{xx,cl2}}}{\epsilon_{xx,\mathrm{co}}}\frac{G}{F_2}W_{e2}\right)\cos U_e + \left(1 - \frac{G^2}{F_1 F_2}\frac{\epsilon_{xx,\mathrm{cl1}}\epsilon_{xx,\mathrm{cl2}}}{\epsilon_{xx,\mathrm{co}}^2}\frac{W_{e1}W_{e2}}{U_e^2}\right)U_e \sin U_e; \quad \text{(C4)}$$

$$D = \frac{\rho^2 k^2 h_2}{F_2 U_o}\left(\frac{G}{F_1}\frac{W_{o1}}{U_o}\sin U_o + \cos U_o\right) + \frac{\rho^2 k^2 h_1}{F_1 U_o}\left(\cos U_e - \frac{\epsilon_{xx,\mathrm{cl2}}}{\epsilon_{xx,\mathrm{co}}}\frac{G}{F_2}\frac{W_{e2}}{U_e}\sin U_e\right); \quad \text{(C5)}$$

ρ is the thickness of the waveguide; k is the free-space propagation constant; and F_i, G, W_{oi}, W_{ei}, U_o, and U_e are defined as in Marcuse's paper:

$$U_o^2 = \rho^2(k^2\epsilon'_{11,\mathrm{co}} - \beta^2), \quad \text{(C6)}$$

$$W_{oi}^2 = \rho^2(\beta^2 - k^2\epsilon'_{11,\mathrm{cli}}), \quad \text{(C7)}$$

$$U_e^2 = \rho^2\left[k^2\epsilon'_{33,\mathrm{co}} - \beta^2\left(\sin^2\alpha + \frac{\epsilon'_{33,\mathrm{co}}}{\epsilon'_{11,\mathrm{co}}}\cos^2\alpha\right)\right], \quad \text{(C8)}$$

$$W_{ei}^2 = \rho^2\left[\beta^2\left(\sin^2\alpha + \frac{\epsilon'_{33,\mathrm{cli}}}{\epsilon'_{11,\mathrm{cli}}}\cos^2\alpha\right) - k^2\epsilon'_{33,\mathrm{cli}}\right], \quad \text{(C9)}$$

$$F_i = W_{oi}^2 \cot^2\alpha - \rho^2 k^2 \epsilon'_{11,\mathrm{cli}}, \quad \text{(C10)}$$

$$G = U_o^2 \cot^2\alpha + \rho^2 k^2 \epsilon'_{11,\mathrm{co}}, \quad \text{(C11)}$$

and h_i is defined as

$$h_i = \epsilon'_{11,\mathrm{co}} W_{oi}^2 + \epsilon'_{11,\mathrm{cli}} U_o^2. \quad \text{(C12)}$$

ACKNOWLEDGMENTS

We gratefully acknowledge useful discussions with R. Black. This research was supported by the U.S. Air Force Office of Scientific Research and the Defense Advanced Research Projects Agency Optoelectronic Materials Center.

REFERENCES

1. A. W. Snyder and F. Ruhl, "Single-mode, single-polarization fibers made of birefringent material," J. Opt. Soc. Am. **73,** 1165–1174 (1983).
2. D. Marcuse and I. P. Kaminov, "Modes of a symmetric slab optical waveguide in birefringent media. Part II: slab with coplanar optical axis," IEEE J. Quantum Electron. **QE-15,** 92–101 (1979).
3. A. Knoesen, T. K. Gaylord, and M. G. Moharam, "Hybrid modes in uniaxial dielectric planar waveguides," IEEE J. Lightwave Technol. **LT-6,** 1083–1103 (1988).
4. D. P. Gia Russo and J. H. Harris, "Wave propagation in anisotropic thin-film optical waveguides," J. Opt. Soc. Am. **63,** 138–145 (1973).
5. W. K. Burns, S. K. Sheem, and A. F. Milton, "Approximate calculation of a leaky-mode loss coefficients for Ti-diffused $LiNbO_3$ waveguides," IEEE J. Quantum Electron. **QE-15,** 1282–1289 (1979).
6. M. Cada, J. Ctyroky, I. Gregora, and J. Schrofel, "WKB analysis of guided and semileaky modes in graded-index anisotropic optical waveguides," Opt. Commun. **28,** 59–63 (1979).
7. S. Yamamoto, Y. Okamura, and T. Makimoto, "Analysis and design of semileaky-type thin-film optical waveguide isolator," IEEE J. Quantum Electron. **QE-12,** 764–770 (1976).
8. K. Yamanouchi, T. Kamiya, and K. Shibayama, "New leaky surface waves in anisotropic metal-diffused optical waveguides," IEEE Trans. Microwave Theory Tech. **MTT-26,** 298–305 (1978).
9. F. F. Ruhl and A. W. Snyder, "Anisotropic fibers studied by the Green's function method," IEEE J. Lightwave Technol. **LT-2,** 284–291 (1984).
10. A. W. Snyder and A. Ankiewicz, "Anisotropic fibers with nonaligned optical (stress) axes," J. Opt. Soc. Am. A **3,** 856–863 (1986).
11. A. W. Snyder and J. D. Love, *Optical Waveguide Theory* (Chapman & Hall, London, 1983), pp. 286–287.
12. A. W. Snyder and F. F. Ruhl, "Anisotropic multimoded fibers," Electron Lett. **19,** 401–402 (1983).
13. P. M. Morse and H. Feshbach, *Methods of Theoretical Physics* (McGraw-Hill, New York, 1953), pp. 884–886.
14. M. J. Adams, *An Introduction to Optical Waveguides* (Wiley, Chichester, UK, 1981), p. 7.
15. D. Marcuse, *Light Transmission Optics* (Van Nostrand Reinhold, New York, 1982), pp. 305–322.
16. D. Marcuse, *Theory of Dielectric Optical Waveguides* (Academic, New York, 1974), pp. 7–26.
17. A. Tonning, "Circular symmetric optical waveguide with strong anisotropy," IEEE Trans. Microwave Theory Tech. **MTT-30,** 790–794 (1982).
18. J. Badan, R. Hierle, A. Perigaud, and P. Vidakovic, in *Nonlinear Optical Properties of Organic Molecules and Crystals,* D. S. Chemla, ed. (Academic, Orlando, Fla., 1987), Chap. 11-4, p. 341.
19. S. Sudo, A. Cordova, R. L. Byer, and H. J. Shaw, "MgO:$LiNbO_3$ single-crystal fiber with magnesium-ion in-diffused cladding," Opt. Lett. **12,** 938–940 (1987).
20. Ref. 14, pp. 126–128.